

DESIGNING OF LOG PERIODIC DIPOLE ANTENNA (LPDA) AND IT'S PERFORMANCE ANALYSIS



Prepared by

Iftekhar Rahman (Student ID: 201116011)

Sunny Md. Shahriar Istiak (Student ID: 201116028)

Syed Aftab Uddin Tonmoy (Student ID: 201116055)

Supervised by

Brig Gen Shaikh Muhammad Rizwan Ali , psc, te

**DEPARTMENT OF ELECTRICAL, ELECTRONIC AND COMMUNICATION
ENGINEERING**

MILITARY INSTITUTE OF SCIENCE AND TECHNOLOGY

DHAKA 1216, BANGLADESH

December 2014

CERTIFICATION

This thesis paper titled “DESIGNING OF LOG PERIODIC DIPOLE ANTENNA (LPDA) AND IT’S PERFORMANCE ANALYSIS” submitted by the group as mentioned below has been accepted as ‘satisfactory’ in partial fulfillment of the requirements for the degree B.Sc. in Electrical, Electronic and Communication Engineering on December 2014.

Supervisor:

Brig Gen Shaikh Muhammad Rizwan Ali , psc, te
Dean,
Faculty of Science & Technology
Bangladesh University of Professionals
Mirpur Cantonment, Dhaka-1216.

DECLARATION

This is to certify that the work presented in this thesis paper titled 'DESIGNING OF LOG PERIODIC DIPOLE ANTENNA (LPDA) AND IT'S PERFORMANCE ANALYSIS' is the yield of study, analysis, simulation and research work carried out by the undersigned group of students of Electrical, Electronic and Communication Engineering (EECE-9), Military Institute Of Science And Technology (MIST), Mirpur Cantonment, under the supervision of Brig Gen Shaikh Muhammad Rizwan Ali, psc, te, Dean, Faculty of Science & Technology, Bangladesh University of Professionals.

It is also declared that neither of this thesis paper nor any part thereof has been submitted anywhere else for the award of any degree, diploma or other qualifications.

Group Members:

Iftekhar Rahman

Student ID: 201116011

Sunny Md. Shahriar Istiak

Student ID: 201116028

Syed Aftab Uddin Tonmoy

Student ID: 201116055

Supervisor:

Brig Gen Shaikh Muhammad Rizwan Ali

Dean

Faculty of Science & Technology

Bangladesh University of Professionals

ACKNOWLEDGEMENT

During past ten months we have had the most fascinating time working on this thesis. So we would like to express our gratitude for the people who made this great time.

We would like to take this opportunity to express our deep and sincere gratitude to our supervisor Brig Gen Shaikh Muhammad Rizwan Ali, psc, te, Dean, Faculty of Science & Technology, BUP throughout the entire work. Above all and the most needed, he provided us unflinching encouragement and support in various ways.

We would also like to thank Lt Col Nazrul, Senior Instructor, EECE Dept., MIST for his helpful suggestions regarding the technological aspects.

We also feel thankful to Lec Moinul Islam, EECE Dept, MIST and our friends for their help.

We, additionally, would like to express our gratitude towards our parents.

Dhaka

21 December, 2014

Iftekhar Rahman

Sunny Md. Shahriar Istiak

Syed Aftab Uddin Tonmoy

ABSTRACT

The introduction of broadband communication system and radar technologies has demanded the design of broadband antennas. One of the major drawbacks with many RF antennas is that they have a relatively small bandwidth. The log periodic antenna is able to provide directivity and gain while being able to operate over a wide bandwidth. The log periodic antenna is used in a number of applications where a wide bandwidth is required along with directivity and a modest level of gain. It is sometimes used on the HF portion of the spectrum where operation is required on a number of frequencies to enable communication to be maintained. It is also used at VHF and UHF for a variety of applications, including some uses as a television antenna. The length and spacing of the elements of a log-periodic antenna increase logarithmically from one end to the other.

Data transmission at higher rates requires wider bandwidths for the elements constituting a communication link. This required wideband antennas to be designed and used. In this thesis, a high gain(around 9dbi) Log Periodic Dipole Antenna of frequency range 1350MHz-2690MHz is designed in order to replace the existing low gain (around 6dbi) corner reflector conical antenna. High Frequency Structure Simulator (HFSS) software is used in the analysis process of the designed LPDA parameters. The design is made in such a way that it can cover maximum area within its frequency range. A physical antenna is also constructed though not tested in the field.

REMARKS

Dept. Head's Remark:

Thesis Supervisor's Remark:

TABLE OF CONTENTS

CERTIFICATION.....	i
DECLARATION.....	ii
ACKNOWLEDGEMENT.....	iii
ABSTRACT.....	iv
REMARKS.....	v
TABLE OF CONTENTS.....	vi
LIST OF FIGURES.....	viii
LIST OF TABLES.....	xi
LIST OF ABBREVIATIONS.....	xii
CHAPTER 1 - INTRODUCTION.....	1
1.1 Research Aim.....	1
1.2 Research Objectives	2
1.3 Methodology.....	2
CHAPTER 2 – UNDERSTANDING ANTENNA PARAMETERS.....	3
2.1 History.....	3
2.2 Antenna Requirements and Specification	4
2.3 Fundamental Antenna Parameters.....	5
2.3.1 Radiation Pattern	5
2.3.2 Beamwidth	7
2.3.3 Directivity	8
2.3.4 Efficiency.....	10
2.3.5 Gain	10
2.3.6 Bandwidth	11
2.3.7 Polarization	12
2.3.8 Friis Transmission Equation.....	12
CHAPTER 3 - THEORY OF LOG-PERIODIC ANTENNA.....	14
3.1 Broadband Antennas.....	14
3.2 Frequency Independent Concept.....	16
3.2.1 Frequency-Independent Planar Log-Spiral Antenna	17
3.2.2 Frequency-Independent Conical-Spiral Antenna	20

3.2.3 The Log-Periodic Antenna	22
3.2.4 The Yagi Yuda Corner Log Periodic Array	27
CHAPTER 4 - FAMILIARIZATION WITH HFSS	30
4.1 Introduction	30
4.2 Working Principle	30
4.3 Boundary Conditions	31
4.4 Technical Definition	32
CHAPTER 5 - DESIGN OF LPDA	35
5.1 Introduction	35
5.2 Design Specifications	37
5.3 Design Calculation	39
CHAPTER 6 – PERFORMANCE ANALYSIS	43
6.1 Design Structure & Simulation Results.....	43
6.2 Radiation Pattern.....	50
6.3 Current Density on the Surface	55
6.4 Output Parameters Calculation	57
CHAPTER 7 – CONCLUSION AND FUTURE WORKS	60
7.1 Conclusion	60
7.2 Future Works.....	60
 BIBLIOGRAPHY.....	 62

LIST OF FIGURES

Figure 2.3a: Dipole model and 3D radiation pattern of antenna	6
Figure 2.3b: Two dimensional radiation plot for half-wave dipole antenna.....	6
Figure 2.3c: Three- and two-dimensional power pattern of antenna.....	8
Figure 2.3d: Geometrical orientation of transmitting and receiving antennas for Friis transmission equation.....	13
Fig 3.1a - Wideband Antenna: Volcano smoke 120° wide-cone-angle bi-conical antenna.....	15
Fig 3.1b - Wideband Antenna: Volcano smoke has end cap with absorber.....	15
Fig 3.1c - Adjustable $\lambda/2$ dipole of 2 drum-type rulers.....	16
Fig 3.2a: The self complementary planar antennas.....	17
Fig 3.2b – Logarithmic or Log spiral Antenna Pattern.....	18
Fig 3.2c: Frequency-independent planar spiral antenna.....	19
Fig 3.2d – Tapered helical or conical-spiral antenna.....	20
Fig 3.2e: Dyson 2-arm balanced conical spiral antenna.....	21
Fig 3.2f: Isbell Log-periodic frequency-independent type of dipole array.....	22
Fig 3.2g: Log-periodic array geometry for determining the relation of parameters.....	23
Fig 3.2h: Relation of Log periodic array parameters.....	24
Fig 3.2i: Construction and feed details of Log-periodic dipole array.....	25
Fig 3.2j: Construction and feed details of Log-periodic dipole array.....	26
Fig 3.2k: Stacked Log-periodic arrays with wire zigzag design.....	26
Fig 3.2l: Stacked Log-periodic arrays with trapezoidal toothed design.....	27
Fig 3.2m: YUCOLP (Yagi-Uda-Corner-Log-Periodic) hybrid array.....	28

Fig 3.2n: Yagi antenna details.....	28
Figure 4.2: HFSS Solution Process.....	31
Figure 5.1: Schematic diagram of log-periodic dipole antenna.....	36
Figure 5.2a: The configuration of a log-periodic antenna and its radiation pattern.....	38
Figure 5.2b: Computed contours of constant directivity versus σ and τ for log-periodic dipole arrays.....	39
Figure 6.1a: LPDA antenna design structure in HFSS Simulation.....	43
Figure 6.1b: LPDA antenna design structure for simulation with radiation box.....	43
Figure 6.1c: Frequency vs. dB(S(1,1)) curve when simulated between 1-3 GHz.....	44
Figure 6.1d: 3-D rectangular plot of Frequency vs. dB(S(1,1)) of LPDA when simulated between 1-3 GHz.....	45
Figure 6.1e: Frequency vs. VSWR curve of designed LPDA.....	45
Figure 6.1f: 3-D rectangular plot of Frequency vs. VSWR of designed LPDA when simulated between 1-3 GHz.....	46
Figure 6.1g: Gain Vs Directivity Curve of designed LPDA	47
Figure 6.1h: Gain(db) vs theta (deg) Curve of designed LPDA	47
Figure 6.1i: Total Gain(db) vs theta (deg) curve at frequency=2.02GHz, phi=0 deg.....	48
Figure 6.1j: Total Gain(db) vs theta (deg) curve at frequency=2.02GHz, phi = 10 deg.....	48
Figure 6.1k: Total Gain(db) vs theta (deg) curve at frequency=2.02GHz, phi=90 deg.....	49
Figure 6.1l: Total Gain(db) vs theta (deg) curve at frequency=2.02GHz, phi=280 deg.....	49

Figure 6.2a: Total Radiation pattern of designed LPDA	50
Figure 6.2b: Radiation Pattern at frequency =2.02GHz, phi=0 deg.....	51
Figure 6.2c: Radiation Pattern at frequency =2.02GHz, phi=60 deg.....	51
Figure 6.2d: Radiation Pattern at frequency =2.02GHz, phi=120 deg.....	52
Figure 6.2e: Radiation Pattern at frequency = 2.02 GHz, phi= 180 deg.....	52
Figure 6.2f: Radiation Pattern at frequency = 2.02 GHz, phi= 240 deg.....	53
Figure 6.2g: Radiation Pattern at frequency = 2.02 GHz, phi= 300 deg.....	53
Figure 6.2h: Radiation Pattern at frequency = 2.02 GHz, phi= 360 deg.....	54
Figure 6.2i: 3-D Radiation pattern of designed LPDA	54
Figure 6.3a: Current density at 1GHz.....	55
Figure 6.3b: Current density at 1.5 GHz.....	55
Figure 6.3c: Current density at 2.02 GHz.....	56
Figure 6.3d: Current density at 2.5 GHz.....	56
Figure 6.5: Physical structure of the designed LPDA	59

LIST OF TABLES

Table 1: Measurement of desired antenna elements	42
Table 2: List of output antenna parameters	57

LIST OF ABBREVIATIONS

BGA= Ball Grid Array
EM= Electromagnetic
EMC= Electromagnetic Compatibility
EMI= Electromagnetic Interference
FEM= Finite Element Method
FNBW= First-Null Beamwidth
FSS= Frequency Selective Surface
HF= High Frequency
HFSS= High Frequency Structure Simulator
HPBW= Half Power Beam Width
LPDA= Log Periodic Dipole Array
PEC= Perfect Electric Conductor
QFP= Quad Flat Package
RCS= Radar Cross Section
RCP= Right Circular Polarized
RF= Radio Frequency
UHF= Ultra High Frequency
VHF= Very High Frequency
VSWR= Voltage Standing Wave ratio
YUCOLP= Yagi Uda Corner Log Periodic

CHAPTER 1

INTRODUCTION

The introduction of broadband system to communication and radar technologies has demanded the design of broadband antennas. As economically and practically it is not possible to make antenna for each band of frequency, Log-Periodic antennas are widely used for applications where a large frequency band is needed. At any frequency, only a small part of the whole structure is active. Electrical properties of a log- periodic antenna such as input impedance, pattern, directivity, side lobe level, beamwidth variations are periodic with the logarithm of the frequency. Antennas obtained from this principle are called log-periodic. Successive dipole lengths, dipole diameters and distance of the successive dipoles from the apex angle α of the antenna are related by the design constant τ . If τ is selected very close to 1, the variations over the frequency band will be small. In practice, even with τ which is not very close to 1, good frequency-independent characteristics are observed. Horn antennas and spiral antennas are the other examples for wide band antennas [1].

The first log-periodic antenna which is bidirectional was introduced by Isbell and DuHammel. Later, Isbell could obtain a unidirectional pattern by using a non planar arrangement of the two halves of the antenna. Then he introduced the most commonly used antenna, log-periodic dipole array.

Log-periodic antennas are important with their ability to show nearly frequency independent characteristics over wide band of frequencies, although they have relatively simple geometries. Numerous different configurations of Log-periodic antennas have been studied since late 1950s. Among them Log-periodic Dipole Antenna has been most popular. Frequency independence of Log-periodic antennas is based on strictly theoretical principles, which is difficult to satisfy in practical implementations.

Bangladesh Army is using corner reflector conical antenna of range 1350-2690 MHz which is one kind of broadband antenna. But that type of antenna is bulky and communication range is small due to its low dBi (around 6 dBi). In this thesis, we have tried to design a physically light but high gain (around 9dBi) LPDA so that it can cover maximum distance range.

1.1 Research Aim

The aims of the research are:

- a) To design a log periodic dipole antenna of high gain in place of existing conical antenna.

- b) To simulate the designed log periodic antenna.
- c) To construct the designed antenna.

1.2 Research Objectives

The objectives of this research are:

- a) To investigate high gain log periodic dipole antenna design methods.
- b) To model and simulate the LPDA.
- c) To construct and measure all the characteristics of the LPDA and to make necessary improvements on the antenna.
- d) To test the antenna physically and analyze the characteristics with its simulated result.

1.3 Methodology

For designing LPDA, first the parameters of LPDA were calculated. Then the designed antenna was simulated using HFSS software. The operating frequency of the antenna is 1350-2690 MHz. The scaling factor is 0.93 and spacing factor is 0.16. The numbers of elements were eleven. One additional element was added for safety issue. Thus total numbers of elements were twelve. Finally a physical antenna was built using copper element.

CHAPTER 2

UNDERSTANDING ANTENNA PARAMETERS

2.1 History

The history of antennas [2] dates back to James Clerk Maxwell who unified the theories of electricity and magnetism, and eloquently represented their relations through a set of profound equations best known as Maxwell's Equations. His work was first published in 1873 [3]. He also showed that light was electromagnetic and that both light and electromagnetic waves travel by wave disturbances of the same speed. In 1886, Professor Heinrich Rudolph Hertz demonstrated the first wireless electromagnetic system. He was able to produce in his laboratory at a wavelength of 4 m a spark in the gap of a transmitting $\lambda/2$ dipole which was then detected as a spark in the gap of a nearby loop. It was not until 1901 that Guglielmo Marconi was able to send signals over large distances. He performed, in 1901, the first transatlantic transmission from Poldhu in Cornwall, England, to St. John's Newfoundland. His transmitting antenna consisted of 50 vertical wires in the form of a fan connected to ground through a spark transmitter. The wires were supported horizontally by a guyed wire between two 60-m wooden poles. The receiving antenna at St. John's was a 200-m wire pulled and supported by a kite. This was the dawn of the antenna era.

From Marconi's inception through the 1940s, antenna technology was primarily centered on wire related radiating elements and frequencies up to about UHF. It was not until World War II that modern antenna technology was launched and new elements (such as waveguide apertures, horns, reflectors) were primarily introduced. Much of this work is captured in the book by Silver [4]. A contributing factor to this new era was the invention of microwave sources (such as the klystron and magnetron) with frequencies of 1 GHz and above.

While World War II launched a new era in antennas, advances made in computer architecture and technology during the 1960s through the 1990s have had a major impact on the advance of modern antenna technology, and they are expected to have an even greater influence on antenna engineering into the twenty-first century. Beginning primarily in the early 1960s, numerical methods were introduced that allowed previously intractable complex antenna system configurations to be analyzed and designed very accurately. In addition, asymptotic methods for both low frequencies (e.g., Moment Method (MM), Finite-Difference, Finite-Element) and high frequencies (e.g., Geometrical and Physical Theories of Diffraction) were introduced, contributing significantly to the maturity of the antenna field. While in the past antenna design may have

been considered a secondary issue in overall system design, today it plays a critical role. In fact, many system successes rely on the design and performance of the antenna. Also, while in the first half of this century antenna technology may have been considered almost a “cut and try” operation, today it is truly an engineering art. Analysis and design methods are such that antenna system performance can be predicted with remarkable accuracy. In fact, many antenna designs proceed directly from the initial design stage to the prototype without intermediate testing. The level of confidence has increased tremendously.

Prior to World War II most antenna elements were of the wire type (long wires, dipoles, helices, rhombuses, fans, etc.), and they were used either as single elements or in arrays. During and after World War II, many other radiators, some of which may have been known for some and others of which were relatively new, were put into service. This created a need for better understanding and optimization of their radiation characteristics. Many of these antennas were of the aperture type (such as open-ended waveguides, slots, horns, reflectors, lenses), and they have been used for communication, radar, remote sensing, and deep space applications both on airborne and earth-based platforms. Prior to the 1950s, antennas with broadband pattern and impedance characteristics had bandwidths not much greater than about 2:1. In the 1950s, a breakthrough in antenna evolution was created which extended the maximum bandwidth to as great as 40:1 or more. Because the geometries of these antennas are specified by angles instead of linear dimensions, they have ideally an infinite bandwidth. Therefore, they are referred to as *frequency independent*. These antennas are primarily used in the 10–10,000 MHz region in a variety of applications including TV, point-to-point communications, feeds for reflectors and lenses, and many others. Major advances in millimeter wave antennas have been made in recent years, including integrated antennas where active and passive circuits are combined with the radiating elements in one compact unit (monolithic form).

2.2 Antenna Requirements and Specification

In order to understand the challenges that LPDA provides to antenna designers, a comprehensive background outlining several characterizing antenna parameters will be presented. Next, a clear description of the challenging that LPDA imposes with regard to these fundamental antenna parameters will be presented requirements. Several parameters have been defined in order to characterize antennas and determine optimal applications. One very useful reference is the IEEE Standard Definitions of Terms for Antennas [5].

Several factors are considered in the simulation, design and testing of an antenna, and most of these metrics are described in 2.3, Fundamental Antenna Parameters. These parameters must be fully defined and explained before a

thorough understanding of antenna requirements for a particular application can be achieved.

2.3 Fundamental Antenna Parameters

Among the most fundamental antenna parameters are radiation pattern, directivity, efficiency and gain. Other characterizing parameters that will be discussed are bandwidth, half-power beamwidth, polarization and range. All of the aforementioned antenna parameters are necessary to fully characterize an antenna and determine whether an antenna is optimized for a certain application.

2.3.1 Radiation Pattern

One of the most common descriptors of an antenna is its radiation pattern. Radiation pattern can easily indicate an application for which an antenna will be used. For example, cell phone use would necessitate a nearly omnidirectional antenna, as the user's location is not known. Therefore, radiation power should be spread out uniformly around the user for optimal reception. However, for satellite applications, a highly directive antenna would be desired such that the majority of radiated power is directed to a specific, known location. According to the IEEE Standard Definitions of Terms for Antennas [5], an antenna radiation pattern (or antenna pattern) is defined as follows:

“A mathematical function or a graphical representation of the radiation properties of the antenna as a function of space coordinates. In most cases, the radiation pattern is determined in the far-field region and is represented as a function of the directional coordinates. Radiation properties include power flux density, radiation intensity, field strength, directivity phase or polarization.”

Three dimensional radiation patterns can be measured on a spherical coordinate system indicating relative strength of radiation power in the far field sphere surrounding the antenna. On the spherical coordinate system, the x-z plane (θ measurement where $\phi=0^\circ$) usually indicates the elevation plane, while the x-y plane (ϕ measurement where $\theta=90^\circ$) indicates the azimuth plane. Typically, the elevation plane will contain the electric-field vector (E-plane) and the direction of maximum radiation, and the azimuth plane will contain the magnetic-field vector (H-Plane) and the direction of maximum radiation. A two-dimensional radiation pattern is plotted on a polar plot with varying ϕ or θ for a fixed value of θ or ϕ , respectively. Figure 2.3a illustrates a half-wave dipole and its three dimensional radiation pattern. The gain is expressed in dBi, which means that the gain is referred to an isotropic radiator. Figure 2.3b illustrates the two dimensional radiation patterns for varying θ at $\phi=0^\circ$, and varying ϕ at $\theta=90^\circ$, respectively. It can be seen quite clearly in Figure 2.3a that the maximum radiation power occurs along the $\theta=90^\circ$ plane, or for any varying ϕ in the azimuth plane. The nulls in the radiation pattern occur at the ends of the

dipole along the z-axis (or at $\theta=0^\circ$ and 180°). By inspection, the two dimensional polar plots clearly show these characteristics, as well. Figure 2.3b shows the radiation pattern of the antenna as the value in the azimuth plane is held constant and the elevation plane (θ) is varied (left), and to the right, it shows the radiation pattern of the antenna as the value in the elevation plane is held constant (in the direction of maximum radiation, $\theta=90^\circ$) as ϕ varies, and no distinction in the radiation pattern is discernable.

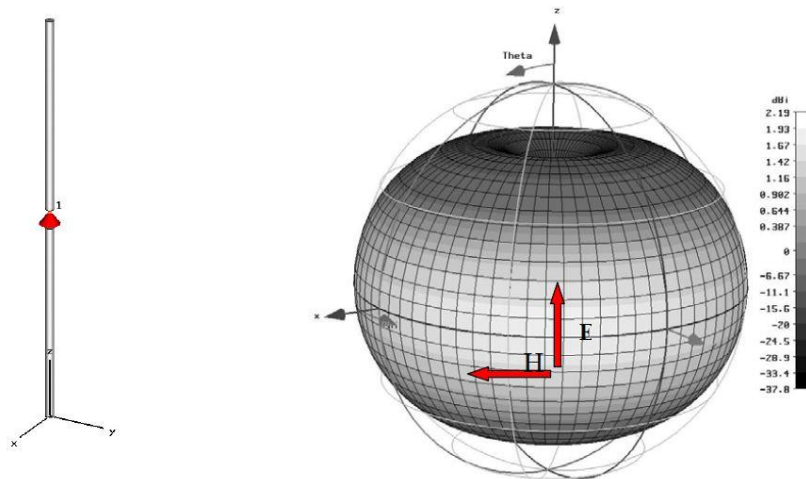


Figure 2.3a: Dipole model and 3D radiation pattern of antenna

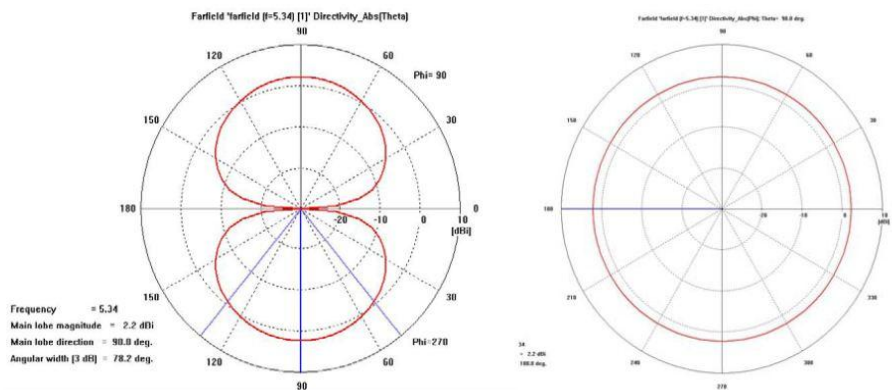


Figure 2.3b: Two dimensional radiation plot for half-wave dipole.

While many two-dimensional radiation patterns are required for a fully complete picture of the three-dimensional radiation pattern, the two most important measurements are the E-plane and H-plane patterns. The E-plane is the plane containing the electric field vector and direction of maximum radiation and the H-plane is the plane containing the magnetic field vector and direction of maximum radiation. While Figure 2.3b shows simply two “cuts” of the antenna radiation pattern, the three-dimensional pattern can clearly be inferred from these two-dimensional illustrations.

The patterns and model in Figure 2.3a and Figure 2.3b illustrate the radiation characteristics of a half-wavelength dipole, which is virtually considered an omnidirectional radiator. The only true omni-directional radiator is that of an isotropic source, which exists only in theory. The IEEE Standard Definitions of Terms for Antennas defines an isotropic radiator as “a hypothetical lossless antenna having equal radiation in all directions.” A true omnidirectional source would have no nulls in its radiation pattern, and therefore have a directivity measurement of 0 dBi. However, since no source in nature is truly isotropic, a directive antenna typically refers to an antenna that is more directive than the half-wave dipole of the figures above.

2.3.2 Beamwidth

Associated with the pattern of an antenna is a parameter designated as beamwidth. The beamwidth of a pattern is defined as the angular separation between two identical points on opposite side of the pattern maximum. In an antenna pattern, there are a number of beamwidths. One of the most widely used beamwidths is the Half-Power Beamwidth (HPBW), which is defined by IEEE as: “In a plane containing the direction of the maximum of a beam, the angle between the two directions in which the radiation intensity is one-half value of the beam.” Another important beamwidth is the angular separation between the first nulls of the pattern, and it is referred to as the First-Null Beamwidth (FNBW). Both the HPBW and FNBW are demonstrated for the pattern in Figure 2.3c. Other beamwidths are those where the pattern is -10 dB from the maximum, or any other value. However, in practice, the term beamwidth, with no other identification, usually refers to HPBW[6].

The beamwidth of an antenna is a very important figure of merit and often is used as a trade-off between it and the side lobe level; that is, as the beamwidth decreases, the side lobe increases and vice versa. In addition, the beamwidth of the antenna is also used to describe the resolution capabilities of the antenna to distinguish between two adjacent radiating sources or radar targets.

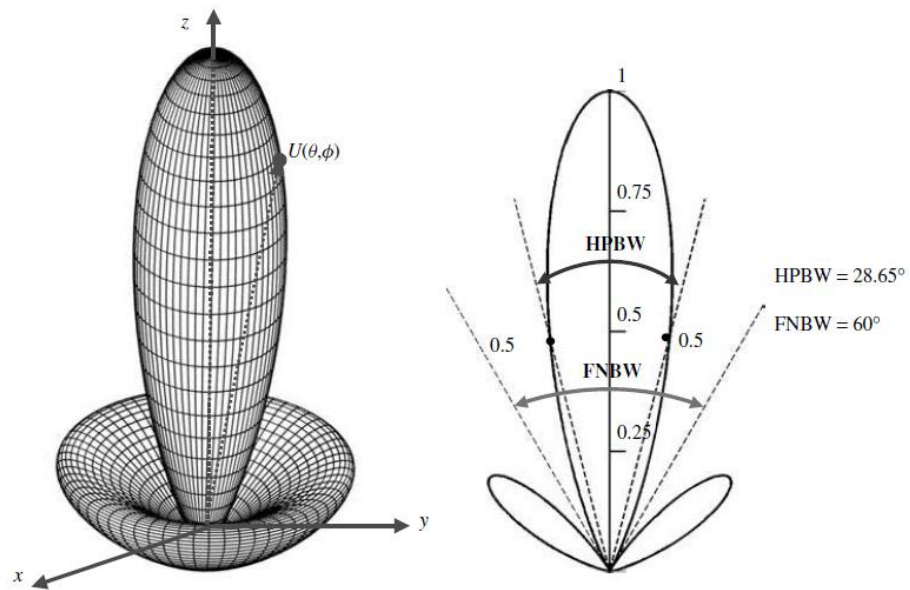


Figure 2.3c: Three- and two-dimensional power patterns (in linear scale)

The most common resolution criterion states that the resolution capability of an antenna to distinguish between two sources is equal to half the first-null beamwidth (FNBW/2), which is usually used to approximate the halfpower beamwidth (HPBW) [7]. That is, two sources separated by angular distances equal or greater than $\text{FNBW}/2 \approx \text{HPBW}$ of an antenna with a uniform distribution can be resolved. If the separation is smaller, then the antenna will tend to smooth the angular separation distance.

2.3.3 Directivity

The directivity of an antenna is defined as “the ratio of the radiation intensity in a given direction from the antenna to the radiation intensity averaged over all directions. The average radiation intensity is equal to the total power radiated by the antenna divided by 4π .” Directivity is more thoroughly understood theoretically when an explanation of radiation power density, radiation intensity and beam solid angle are given.

The average radiation power density is expressed as follows:

$$S_{\text{av}} = \frac{1}{2} \text{Re}[\vec{E} \times \vec{H}^*] \text{ (W/m}^2\text{)} \quad (2.1)$$

Since S_{av} is the average power density, the total power intercepted by a closed surface can be obtained by integrating the normal component of the average

power density over the entire closed surface. Then, the total radiated power is given by the following expression:

$$P_{\text{rad}} = P_{\text{av}} = \frac{1}{2} \oint_S \text{Re} (\vec{E} \times \vec{H}^*) \cdot d\vec{s} = \oint_S S_{\text{rad}} \cdot d\vec{s} \quad (2.2)$$

Radiation intensity is defined by the IEEE Standard Definitions of Terms for Antennas as “the power radiated from an antenna per unit solid angle.” The radiation intensity is simply the average radiation density, S_{rad} , scaled by the square product of the distance, r . This is also a far field approximation, and is given by:

$$U = r^2 S_{\text{rad}} \quad (2.3)$$

Where U = radiation intensity (W/unit solid angle) and S_{rad} = radiation density (W/m²).

The total radiated power, P_{rad} , can be then be found by integrating the radiation intensity over the solid angle of 4π steradians, given as:

$$P_{\text{rad}} = \oint_{\Omega} U d\Omega = \int_0^{2\pi} \int_0^{\pi} U \sin\theta \, d\theta \, d\phi \quad (2.4)$$

$$P_{\text{rad}} = \oint_{\Omega} U_0 d\Omega = U_0 \oint_{\Omega} d\Omega = 4\pi U_0 \quad (2.5)$$

Where $d\Omega$ is the element of solid angle of a sphere, measured in steradians. A steradian is defined as “a unit of measure equal to the solid angle subtended at the center of a sphere by an area on the surface of the sphere that is equal to the radius squared.” Integration of $d\Omega$ over a spherical area as shown in the equation above yields 4π steradians. Another way to consider the steradian measurement is to consider a radian measurement: The circumference of a circle is $2\pi r$, and there are $(2\pi r/r)$ radians in a circle. The area of a sphere is $4\pi r^2$, and there are $4\pi r^2/r^2$ steradians in a sphere.

The beam solid angle is defined as the subtended area through the sphere divided by r^2 :

$$d\Omega = \frac{dA}{r^2} = \sin\theta \, d\theta \, d\phi \quad (2.6)$$

Given the above theoretical and mathematical explanations of radiation power density, radiation intensity and beam solid angle, a more complete understanding of antenna directivity can be achieved. Directivity is defined mathematically as:

$$D = \frac{U}{U_0} = \frac{4\pi U}{P_{\text{rad}}} \text{ (dimensionless)} \quad (2.7)$$

Simply stated, antenna directivity is a measure of the ratio of the radiation intensity in a given direction to the radiation intensity that would be output from an isotropic source.

2.3.4 Efficiency

The antenna efficiency takes into consideration the ohmic losses of the antenna through the dielectric material and the reflective losses at the input terminals. Reflection efficiency and radiation efficiency are both taken into account to define total antenna efficiency. Reflection efficiency, or impedance mismatch efficiency, is directly related to the S_{11} parameter (Γ). Reflection efficiency is indicated by e_r , and is defined mathematically as follows:

$$e_r = (1 - |\Gamma|^2) = \text{reflection efficiency} \quad (2.8)$$

The radiation efficiency takes into account the conduction efficiency and dielectric efficiency, and is usually determined experimentally with several measurements in an anechoic chamber. Radiation efficiency is determined by the ratio of the radiated power, P_{rad} to the input power at the terminals of the antenna, P_{in} :

$$e_{\text{rad}} = \frac{P_{\text{rad}}}{P_{\text{in}}} = \text{radiation efficiency} \quad (2.9)$$

Total efficiency is simply the product of the radiation efficiency and the reflection efficiency.

$$\text{Total Efficiency} = e_{\text{rad}} \times e_r$$

2.3.5 Gain

The antenna gain measurement is linearly related to the directivity measurement through the antenna radiation efficiency. According to the antenna absolute gain is “the ratio of the intensity, in a given direction, to the radiation intensity that would be obtained if the power accepted by the antenna were radiated isotropically.” Antenna gain is defined mathematically as follows:

$$G = e_{\text{rad}} D = 4\pi \frac{U(\theta, \varphi)}{P_{\text{in}}} \quad (\text{dimensionless}) \quad (2.10)$$

Also, if the direction of the gain measurement is not indicated, the direction of maximum gain is assumed. The gain measurement is referred to the power at

the input terminals rather than the radiated power, so it tends to be a more thorough measurement, which reflects the losses in the antenna structure.

Gain measurement is typically misunderstood in terms of determining the quality of an antenna. A common misconception is that the higher the gain, the better the antenna. This is only true if the application requires a highly directive antenna. Since gain is linearly proportional to directivity, the gain measurement is a direct indication of how directive the antenna is (provided the antenna has adequate radiation efficiency).

2.3.6 Bandwidth

The bandwidth of an antenna is defined as “the range of frequencies within which the performance of the antenna, with respect to some characteristic, conforms to a specified standard.” The bandwidth can be considered to be the range of frequencies, on either side of a center frequency (usually the resonance frequency for a dipole), where the antenna characteristics (such as input impedance, pattern, beamwidth, polarization, side lobe level, gain, beam direction, radiation efficiency) are within an acceptable value of those at the center frequency. For broadband antennas, the bandwidth is usually expressed as the ratio of the upper-to-lower frequencies of acceptable operation. For example, a 10:1 bandwidth indicates that the upper frequency is 10 times greater than the lower. For narrowband antennas, the bandwidth is expressed as a percentage of the frequency difference (upper minus lower) over the center frequency of the bandwidth. For example, a 5% bandwidth indicates that the frequency difference of acceptable operation is 5% of the center frequency of the bandwidth [8].

Because the characteristics (input impedance, pattern, gain, polarization, etc.) of an antenna do not necessarily vary in the same manner or are even critically affected by the frequency, there is no unique characterization of the bandwidth. The specifications are set in each case to meet the needs of the particular application. Usually there is a distinction made between pattern and input impedance variations. Accordingly pattern bandwidth and impedance bandwidth are used to emphasize this distinction. Associated with pattern bandwidth are gain, side lobe level, beamwidth, polarization, and beam direction while input impedance and radiation efficiency are related to impedance bandwidth. For example, the pattern of a linear dipole with overall length less than a half-wavelength ($l < \lambda/2$) is insensitive to frequency. The limiting factor for this antenna is its impedance, and its bandwidth can be formulated in terms of the Q. The Q of antennas or arrays with dimensions large compared to the wavelength, excluding superdirective designs, is near unity. Therefore the bandwidth is usually formulated in terms of beamwidth, side lobe level, and pattern characteristics. For intermediate length antennas, the bandwidth may be limited by either pattern or impedance variations, depending upon the particular application. For these antennas, a 2:1 bandwidth indicates a good design. For others, large bandwidths are needed. Antennas

with very large bandwidths (like 40:1 or greater) have been designed in recent years. These are known as frequency independent antennas.

The above discussion presumes that the coupling networks (transformers, baluns, etc.) and/or the dimensions of the antenna are not altered in any manner as the frequency is changed. It is possible to increase the acceptable frequency range of a narrowband antenna if proper adjustments can be made on the critical dimensions of the antenna and/or on the coupling networks as the frequency is changed. Although not an easy or possible task in general, there are applications where this can be accomplished. The most common examples are the antenna of a car radio and the “rabbit ears” of a television. Both usually have adjustable lengths which can be used to tune the antenna for better reception.

2.3.7 Polarization

Antenna polarization indicates the polarization of the radiated wave of the antenna in the far-field region. The polarization of a radiated wave is the property of an electromagnetic wave describing the time varying direction and relative magnitude of the electric-field vector at a fixed location in space, and the sense in which it is traced, as observed along the direction of propagation [4]. Typically, this is measured in the direction of maximum radiation. There are three classifications of antenna polarization: linear, circular and elliptical. Circular and linear polarizations are special cases of elliptical polarization. Typically, antennas will exhibit elliptical polarization to some extent. Polarization is indicated by the electric field vector of an antenna oriented in space as a function of time. Should the vector follow a line, the wave is linearly polarized. If it follows a circle, it is circularly polarized (either with a left hand sense or right hand sense). Any other orientation is said to represent an elliptically polarized wave. Aside from the type of polarization, two main factors are taken into consideration when considering polarization of an antenna: Axial ratio and polarization mismatch loss.

2.3.8 Friis Transmission Equation

The Friis Transmission Equation relates the power received to the power transmitted between two antennas separated by a distance $R > 2D^2/\lambda$, where D is the largest dimension of either antenna [9]. Referring to Figure 2.3d, let us assume that the transmitting antenna is initially isotropic. If the input power at the terminals of the transmitting antenna is P_t , then its isotropic power density W_0 at distance R from the antenna is

$$W_0 = e_t \frac{P_t}{4\pi R^2} \quad (2.11)$$

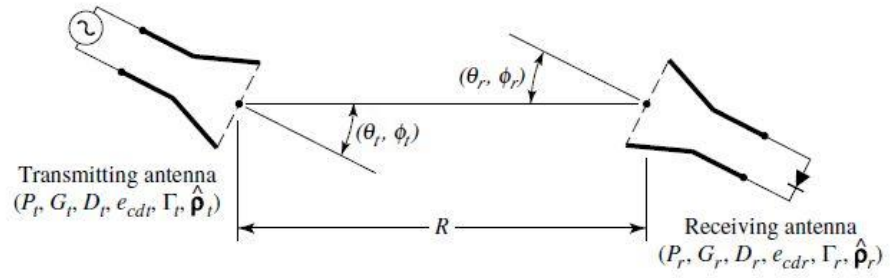


Figure 2.3d: Geometrical orientation of transmitting and receiving antennas for Friis transmission equation.

where e_t is the radiation efficiency of the transmitting antenna. For a non-isotropic transmitting antenna, the power density of in the direction θ_t, φ_t can be written as:

$$W_t = \frac{P_t G_t(\theta_t, \varphi_t)}{4\pi R^2} = e_t \frac{P_t D_t(\theta_t, \varphi_t)}{4\pi R^2} \quad (2.12)$$

Where $G_t(\theta_t, \varphi_t)$ is the gain and $D_t(\theta_t, \varphi_t)$ is the directivity of the transmitting antenna in the direction θ_t, φ_t .

CHAPTER 3

THEORY OF LOG-PERIODIC ANTENNA

Overview of Log Periodic Antennas

In this chapter broadband antennas with their frequency independent concept and the theory of log periodic antenna have been discussed elaborately.

3.1 Broadband Antennas

Many antennas are highly resonant operating over bandwidths of only a few percent. Such "tuned", narrow bandwidths antennas may be entirely satisfactory or even desirable for single-frequency or narrow-band applications. In many situations, however, wider bandwidth may be required. The volcano smoke unipole antenna of fig 3.1a and the twin Alpine horn antenna of Fig 3.1b are examples of basic wide-bandwidth antennas. The gradual, smooth transition from coaxial or twin line to a radiating structure can provide almost constant input impedance very wide bandwidths. The high frequency limit of the Alpine horn antenna may be said to occur when the transmission-line spacing $d > \lambda/10$ and the low-frequency limit when the open end spacing $D < \lambda/2$. Thus if $D = 1000d$, the antenna has a theoretical 200 to 1 bandwidth. A compact version of the twin Alpine horn, shown in Fig 3.1c has a double ridge waveguide as the launcher on an exponentially honing 2-conductor balanced transmission line.

The design in Fig 3.1c incorporates features used by Kcrr and by Baker and Van der Neut. The exponential taper is of the form

$$y = k_1 e^{k_2 x} \quad (3.1)$$

where k_1 and k_2 are constants. The exact curvature is not critical provided it is gradual. The fields are bound sufficiently close to the ridges that the horn beyond the launcher may be omitted. The version shown is a compromise with the top and bottom of the horn present but solid sides replaced by a grid of conductors with a spacing of about $\lambda/10$ at the lowest frequency. The grid reduces the pattern width in the H-plane and increases the low-frequency gain. The Chuang-Burnside cylindrical end sections on the ridges reduce the back radiation and VSWR. Absorber on the top and bottom of the ridges (or horn) also reduces back-radiation and VSWR.

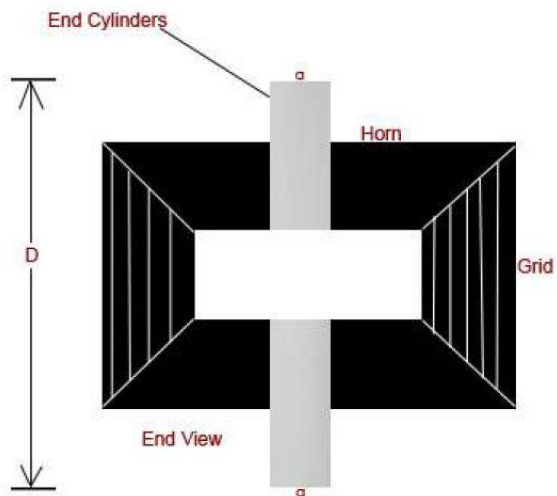


Fig 3.1a: Wideband Antenna: Volcano smoke 120° wide-cone-angle bi-conical antenna

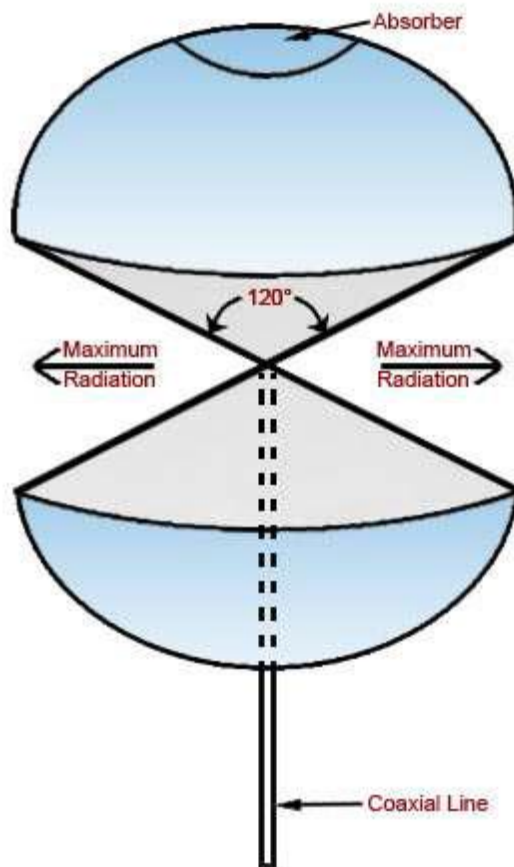


Fig 3.1b: Wideband Antenna: Volcano smoke has end cap with absorber

Depending on the ratio of the open end dimension D to the spacing d of the ridges at the feed end, almost arbitrarily large bandwidths are possible with gain increasing with frequency. Thus, for the antenna of Fig. 3.1c, the feed dimension $d = 1.5$ mm, so that the shortest wavelength $\lambda = 15$ mm ($\lambda/10 = 1.5$ mm) and the open-end dimension $D = 128$ mm so that the longest wavelength $\lambda = 256$ mm ($\lambda/2 = 128$ mm) for a bandwidth of 17 to 1 ($=256/15$). For a similar antenna without end cylinders Kerr reports bandwidths of 17 to 1 with gains up to 14 dBi.

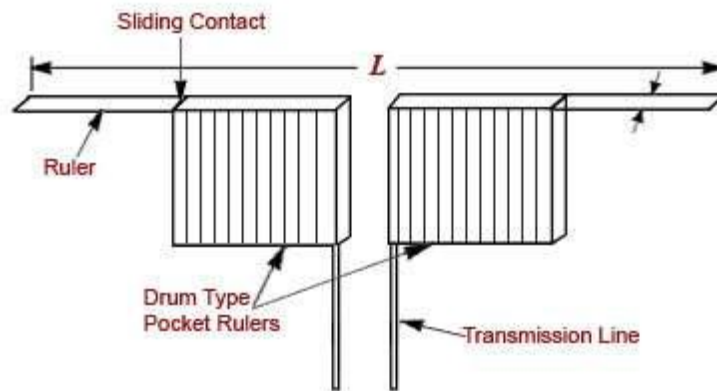


Fig 3.1c: Adjustable $\lambda/2$ dipole of 2 drum-type rulers illustrates the requirement that to be frequency independent an antenna must expand or contract in proportion to the wavelength [10]

The design of Fig 3.1c is linearly polarized (vertical). With two orthogonal sets of ridges forming a quadruply ridged waveguide-fed horn, either vertical or horizontal or circular polarization can be obtained.

3.2 Frequency Independent Concept

RUMSEY'S PRINCIPLE

Rumsey's principle is that the impedance and pattern properties of an antenna will be frequency independent if the antenna shape is specified only in terms of angles. Thus, an infinite logarithmic spiral should meet the requirement.

The bi-conical antenna is an example of an antenna that can be specified only in terms of the included cone angle, but it is frequency independent only if it is infinitely long. When truncated (without a matched termination) there is a reflected wave from the ends of the cones which results in modified impedance and pattern characteristics [11].

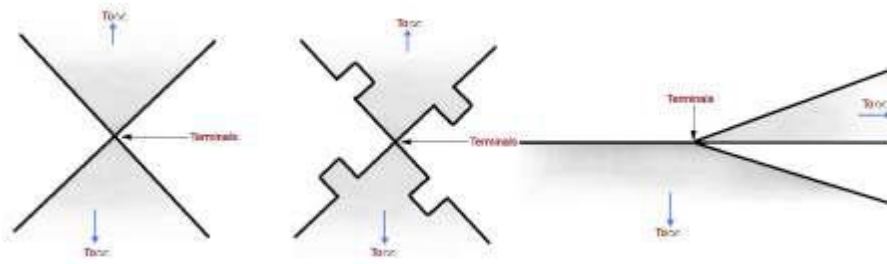


Fig 3.2a: The self complementary planar antennas. Theoretical terminal impedance is 188Ω .

To meet the frequency-independent requirement in a finite structure requires that the current attenuate along the structure and be negligible at the point of truncation. For radiation and attenuation to occur charge must be accelerated (or decelerated) and this happens when a conductor is curved or bent normally to the direction in which the charge is travelling. Thus, the curvature of a spiral results in radiation and attenuation so that, even when truncated. The spiral provides frequency-independent operation over a wide bandwidth [10].

Rumsey's principle was implemented experimentally by John D. Dyson at the University of Illinois. He constructed the first practical frequency-independent spiral antennas in 1958, first the bidirectional planar spiral and then the unidirectional conical spiral.

3.2.1 Frequency-Independent Planar Log-Spiral Antenna

The equation for a logarithmic (or log) spiral is given by

$$r = a^\theta \quad (3.2)$$

$$\text{Or, } \ln r = \theta \ln a \quad (3.3)$$

Where referring to fig 3.2b,

r = radial distance to point P on spiral,
 θ = angle with respect to x axis,
 a = a constant.

From (3.2), the rate of change of radius with angle is

$$\frac{dr}{d\theta} = a^\theta \ln a = r \ln a \quad (3.4)$$

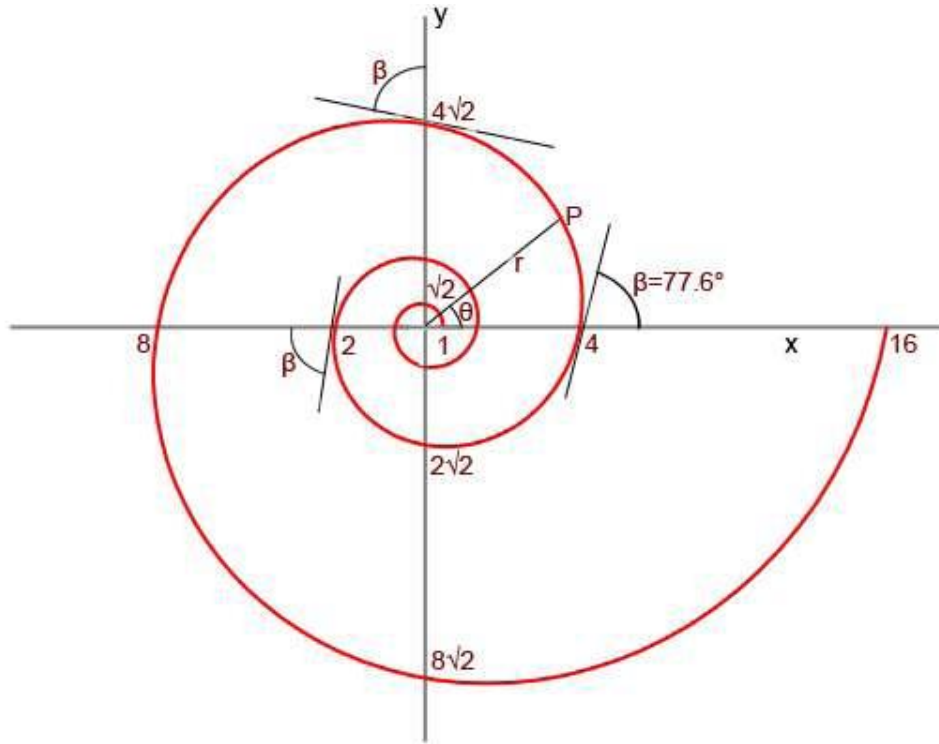


Fig 3.2b: Logarithmic or Log spiral Antenna Pattern

The constant a in (3.4) related to the angle β between the spiral and a radial line from the origin as given by

$$\ln a = \frac{dr}{d\theta} = 1/(\tan \beta) \quad (3.5)$$

Thus from (3.5) and (3.3),

$$\Theta = \tan \beta \ln r \quad (3.6)$$

The log spiral was constructed in fig 3.2c so as to make $r = 1$ and $\Theta = 0$ and $r = 2$ and $\Theta = \pi$.

These conditions determine the value of constants a and β . Thus from (3.5) and (3.6), $\beta = 77.6^\circ$ and $a = 1.247$. Thus the shape of spiral is determined by the angle β which is same for all points on the spiral. Let a second log spiral identical in form to the one in fig 3.2c be generated by an angular rotation δ so that (3.2) becomes

$$r_2 = a^{\Theta - \delta} \quad (3.7)$$

And a third and fourth spiral given by,

$$r_3 = a^{\Theta-\pi} \quad (3.8)$$

$$r_4 = a^{\Theta-\pi-\delta} \quad (3.9)$$

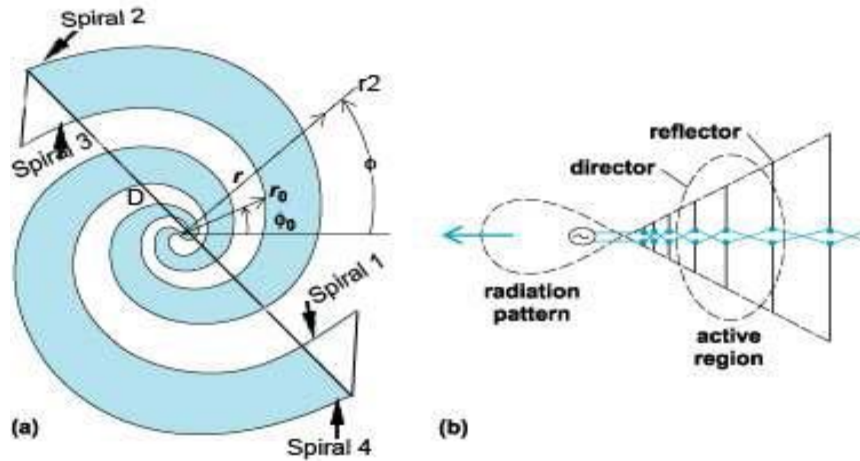


Fig 3.2c: Frequency-independent planar spiral antenna

Then for a rotation $\delta = \pi/2$ we have 4 spirals at 90° angles. Metalizing the areas between spiral 1 and 4 and 2 and 3 with other areas open self complementary and congruence conditions are satisfied. Connecting a generator or receiver across the inner terminals, we obtain Dyson's frequency-independent planar spiral antenna of fig 3.2c. The arrows indicate the directions of the outgoing waves travelling along the conductors resulting in right circularly polarized (RCP) radiation (IEEE definition) outward from the page and left circularly polarized radiation into the page. The high-frequency limit of operation is determined by the spacing d of the input terminal and the low-frequency limit by the overall diameter D . The ratio D/d for the antenna of Fig 3.2c is about 25 to 1. If we take $d = \lambda/10$ at the high-frequency limit and $D = \lambda/2$ at the low-frequency limit, the antenna band-width is 5 to 1. The spiral should be continued to a smaller radius but, for clarity, the terminal separation shown in Fig, 3.2c is larger than it should be. Halving it doubles the bandwidth. In practice it is more convenient to cut the slots for the antenna from a large ground plane, as done by Dyson, and feed the antenna with a coaxial cable bonded to one of the spiral arms as in Fig. 3.2c, the spiral acting as a balun. A dummy cable may be bonded to the other arm for symmetry but is not shown. Radiation for the antenna of Fig. 3.2c is bidirectional broadside to the plane of the spiral. The patterns in both directions have a single broad lobe so that the gain is only a few dBi. The input impedance depends on the parameters δ and

a the terminal separation According to Dyson, typical values are in the range 50 to 100 N, or considerably less than the theoretical $188 N (Z0/2)$. The smaller measured values are apparently due to the finite thickness of spirals [10].

Referring to Fig. 3.2c, the ratio K of the radii across any arm, such as between spirals 2 and 3, is given by the ratio of (3.8) to (3.7), or

$$K = \frac{r_3}{r_2} = a^{-n+\delta} \quad (3.10)$$

For the antenna fig 3.2c, $\delta = \pi/2$ so,

$$K = \frac{r_3}{r_2} = a^{-\pi/2} = 0.707 = 1/\sqrt{2} \quad (3.11)$$

This is seen to be the ratio of the radial distances to the spiral of fig 3.2c at successive 90° intervals [10].

3.2.2 Frequency-Independent Conical-Spiral Antenna

A tapered helix is a conical-spiral antenna and these were described and investigated extensively in the years following 1947.



Fig 3.2d: Tapered helical or conical-spiral (forward-fire) Cp antennas

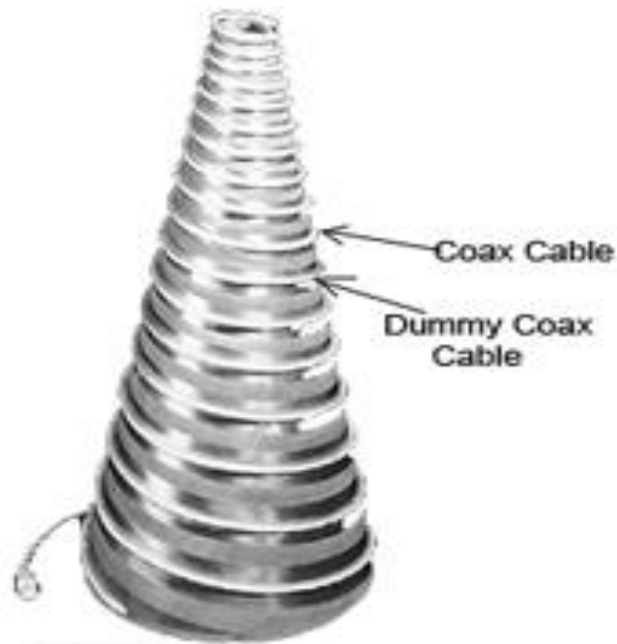


Fig 3.2e: Dyson 2-arm balanced conical spiral (backward-fire) antenna, Polarization is RCP. Inner conductor of coax connects to dummy at apex.

Figure 3.2d and e shows tapered helical or conical spiral antennas in which the pitch angle is constant with diameter and turn spacing variable. However, it was not until 1958 that John D. Dyson at the University of Illinois made the tapered helix or conical spiral fully frequency independent by wrapping or projecting multiple planar spirals onto a conical surface [12]. A typical balanced 2-arm Dyson conical spiral is shown in Fig. 3.2d. The conical spiral retains the frequency-independent properties of the planar spiral while providing broad-lobed unidirectional circularly polarized radiation of the small end or apex of the cone. As with the planar spiral the two arms of the conical spiral are fed at the centre point or apex from a coaxial cable bonded to one of the arms, the spiral acting as a balun. For symmetry a dummy cable may be bonded to the other arm, as suggested in Fig, 3.2d. In some models the metal straps are dispensed with and the cables alone used as the spiral conductors. According to Dyson, the input impedance is between 100 to 150 N for a pitch angle $\alpha = 17^\circ$ and full cone angles of 20 to 60°. The smaller cone angles (30° or less) have higher front-to-back ratios of radiation. The bandwidth as with the planar spiral depends on the ratio of the base diameter ($\sim \lambda/2$ at the lowest frequency) to the truncated apex diameter ($\sim \lambda/4$ at the highest frequency). This ratio may be made arbitrarily large. Conical and planar spirals with more than 2 arms are also possible and have been investigated by Dyson and Mayes and by Deschamps all at the University of Illinois and also by Atai Mei [10].

3.2.3 The Log-Periodic Antenna

While the planar and conical spirals were being developed Raymond Duhamel and Dwight Isbell, also at the University of Illinois created a new type of frequency-independent antenna with a self-complementary toothed structure. In an alternative version the metal and slot areas are interchanged. Since $\beta_1 + \beta_2 = 90^\circ$ the self-complementary condition is fulfilled.

The expansion parameter

$$k_1 = R_{n+1} / R_n \quad (3.12)$$

And the tooth width parameter

$$k_2 = r_n / R_n \quad (3.13)$$

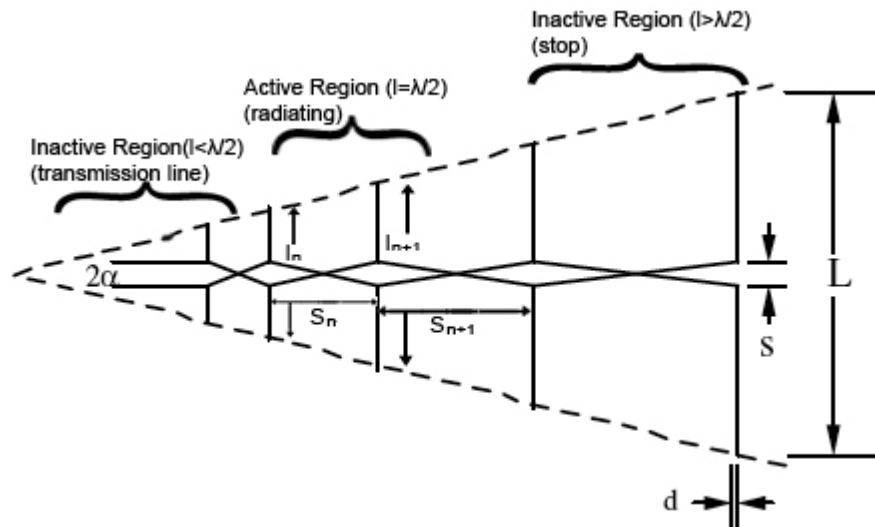


Fig 3.2f: Isbell Log-periodic frequency-independent type of dipole array of 7 dBi gain with 11 dipoles showing active central regions and inactive regions (left and right ends).

Further work at the University of Illinois showed that the self-complementary condition was not required, and by 1960 Dwight Isbell had demonstrated the first log-periodic dipole array. The basic concept is that a gradually expanding periodic structure array radiates most effectively when the array elements (dipoles) are near resonance so that with change in frequency the active (radiating) region moves along the array. This expanding structure array differs

from the uniform arrays considered. The log-periodic dipole array is a popular design. Referring to Fig. 3.2f, the dipole lengths increase along the antenna so that the included angle α is a constant, and the lengths l and spacing s of adjacent elements are scaled so that

$$l_{n+1} / l_n = s_{n+1} / s_n = k \quad (3.14)$$

where k is a constant. At a wavelength near the middle of the operating range, radiation occurs primarily from the central region of the antenna, as suggested in Fig. 3.2f.

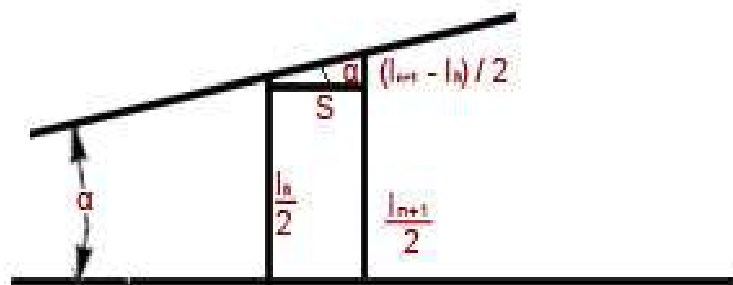


Fig 3.2g: Log-periodic array geometry for determining the relation of parameters.

The elements in this active region are about $\lambda/2$ long. Elements 9, 10 and 11 are in the neighborhood λ long and carry only small currents (they present a large inductive reactance to the line). The small currents in elements 9, 10 and 11 mean that the antenna is effectively truncated at the right of the active region. Any small fields from elements 9, 10 and 11 also tend to cancel in both forward and backward directions. However, some radiation may occur broadside since the currents are approximately in phase. The elements at the left (1, 2, 3, etc.) are less than $\lambda/2$ long and present a large capacitive reactance to the line. Hence, currents in these elements are small and radiation is small.

Thus, at a wavelength λ , radiation occurs from the middle portion where the dipole elements are $\sim \lambda/2$ long. When the wavelength is increased the radiation zone moves to the right and when the wavelength is decreased it moves to the left with maximum radiation toward the apex or feed point of the array [13]. At

any given frequency only a fraction of the antenna is used (where the dipoles are about $\lambda/2$ long). At the short-wavelength limit of the bandwidth only 15 percent of the length may be used. While at the long-wavelength limit a larger fraction is used but still less than 50 percent.

From the geometry of Fig. 3.2g for a section of the array, we have

$$\tan \alpha = (l_{n+1} - l_n) / (2/s) \quad (3.15)$$

Or from (3.14),

$$\tan \alpha = \{[1-(1/k)] [l_{n+1}/2]\}/2 \quad (3.16)$$

Taking $l_{n+1} = \lambda/2$ (when active) we have

$$\tan \alpha = [1-(1/k)]/[4s_\lambda] \quad (3.17)$$

Where α = apex angle

k = scale factor

s_λ = spacing in wavelengths short ward of $\lambda/2$ element

Specifying any 2 of the 3 parameters α , k and s_λ determines the third. The relationship of the 3 parameters is displayed in Fig. 3.2h with the optimum design line (maximum gain for a given of this value scale factor k) and gain along line from calculations of Carrel, Cheong and King, De Vito and Stracca and Buston and Thomson.

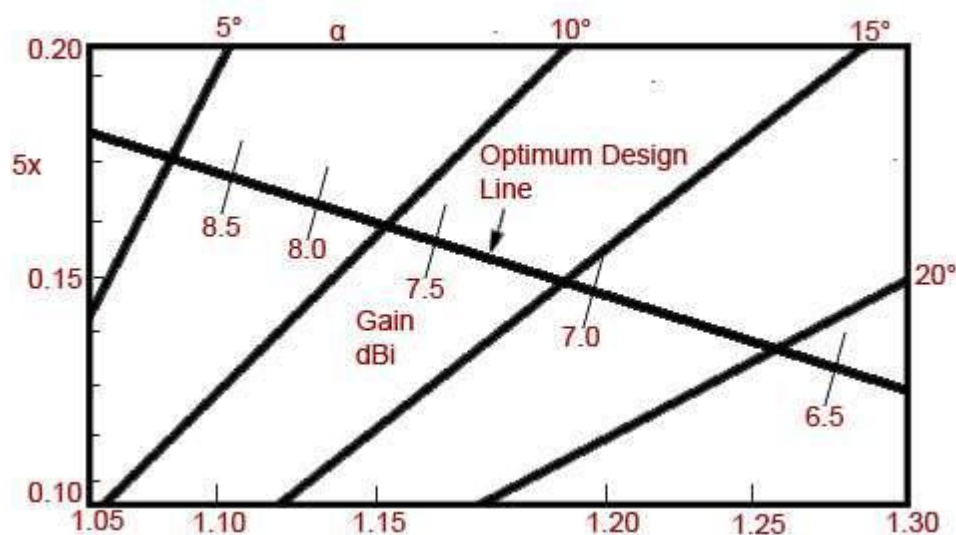


Fig 3.2h: Relation of Log periodic array parameters of apex angle α , scale factor k and spacing s_λ with optimum design line and gain values according to Carrel and others [14].

The length l (and spacing s) for any element $n + 1$ is k^n greater than for element 1, or

$$l_{n+1}/l_1 = k^n = F \quad (3.18)$$

Where F = frequency ratio or bandwidth.

Thus if $k = 1.19$ and $n = 4$, $F = k^4 = 1.19^4 = 2$ and element 5 ($= n + 1$) is twice the length l_1 , of element 1. Thus, with 5 elements and $k = 1.19$, the frequency ratio is 2 to 1.

The array of Fig. 3.2h corresponds to the parameters of the above example. The E-plane HPBW ≈ 60 and the H-plane beam width is a function of the gain is given by

$$\text{HPBW (H plane)} = 41000/(D * 60) \text{ (deg)} \quad (3.19)$$

For the antenna of the example $D = 5$, since $\log_{10} 5 = 0.7$ dBi, so

$$\text{HPBW (H plane)} = 41000/(5 * 60) = 137^\circ \quad (3.20)$$

Details of construction and feeding are shown in Fig. 3.2i. the arrangement in (a) is fed with coaxial cable, the one at (b) with twin line [10].

To obtain more gain than with a single log-periodic dipole array, 2 arrays may be stacked. However, for frequency-independent operation, Rumsey's principle requires that the locations of all elements be specified by angles rather than distances. This means that both log-periodic arrays must have 8 common apexes, and accordingly, the beams of the 2 arrays point in different directions.

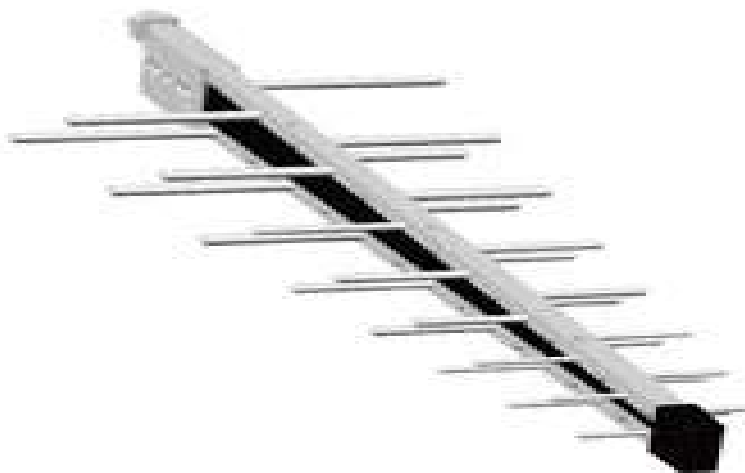


Fig 3.2i: Construction and feed details of Log-periodic dipole array where arrangement is made at 50 or 75 N coaxial feed.

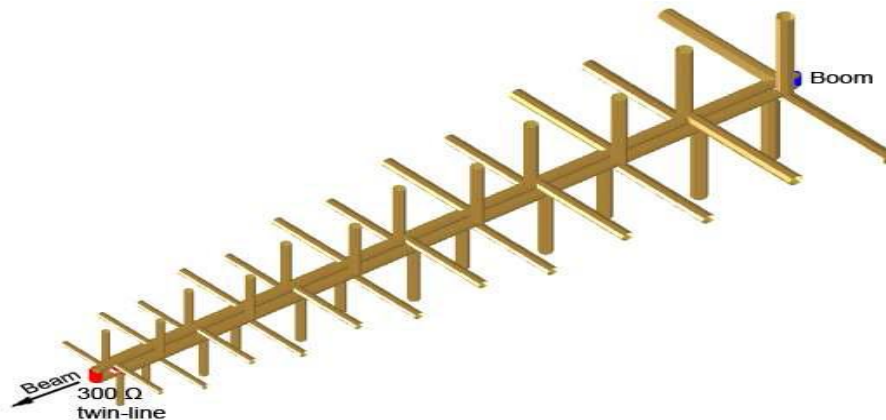


Fig 3.2j: Construction and feed details of Log-periodic dipole array where arrangement is made has criss-crossed open-wire line for 300N twin-line feed.

For a stacking angle of 60° , the situation is as suggested in Fig. 3.2j for dipole arrays of the type shown in Figs. 3.2k and 3.2l. The array in Fig. 3.2l is a skeleton-tooth or edge-fed trapezoidal type. Wires supported by a central boom replace the teeth of the antenna of fig. 3.2j. For very wide bandwidths the log-periodic array must be correspondingly long.

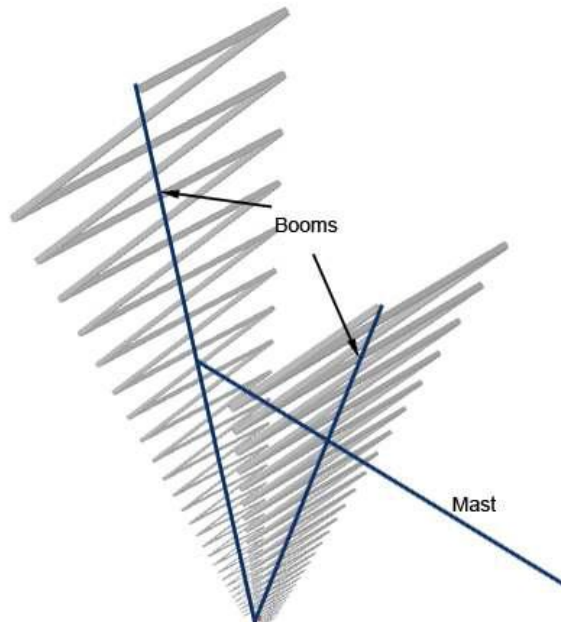


Fig 3.2k: Stacked Log-periodic arrays with wire zigzag design

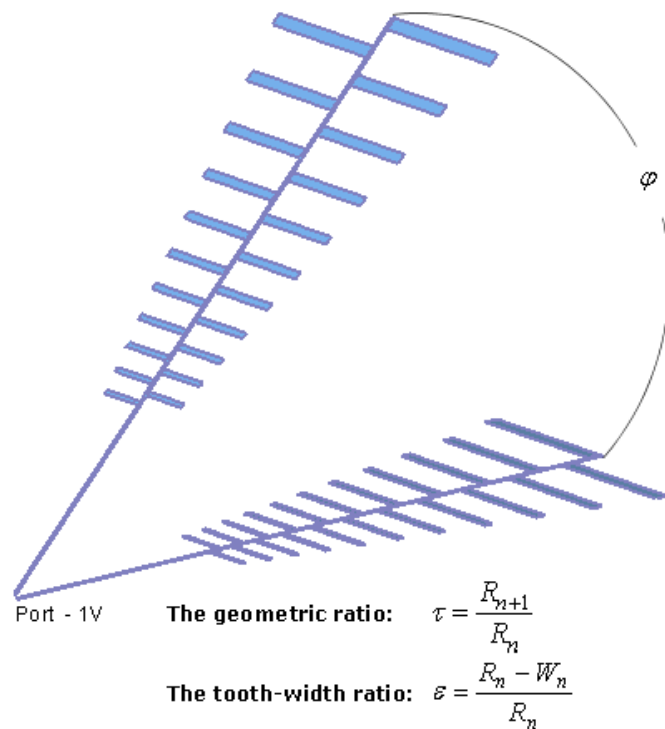


Fig 3.2l: Stacked Log-periodic arrays with trapezoidal toothed design

To shorten the structure, Paul Mayes and Robert Carrel of the University of Illinois, developed a more compact V-dipole array which can operate in several modes. In the lowest mode, with the central region dipoles $\sim \lambda/4$ long operation is as already described. However, as the frequency is increased to the point where the shortest elements are too long to give $\lambda/2$ resonance, the longest elements become active at $3\lambda/2$ resonances. As the frequency is increased further, The active region moves to the small end in the $3\lambda/2$ mode with still further increase in frequency the large end becomes active in still high order modes. The forward tilt of the V-dipoles has little effect on the $\lambda/2$ modes but in the higher modes provides essential forward beaming.

3.2.4 The Yagi Yuda Corner Log Periodic Array

For ultimate compactness and gain, to cover the 54 to 890 MHz TV and FM bands, a hybrid YUCOLP array are a popular design. A typical model, shown in Fig. 3.2m has $\alpha = 43^\circ$. $k = 1.3$ LP array of 5 V-dipoles to cover the 54 to 108 MHz TV and FM bands with a 6 dBi gain in the $\lambda/2$ mode, the 174 to 216 MHz band with 8 or 9 dBi gain in the $3\lambda/2$ mode and a square-corner-YU array to cover the 470 to 890 UHF TV band with a 7 to 10 dBi gain.

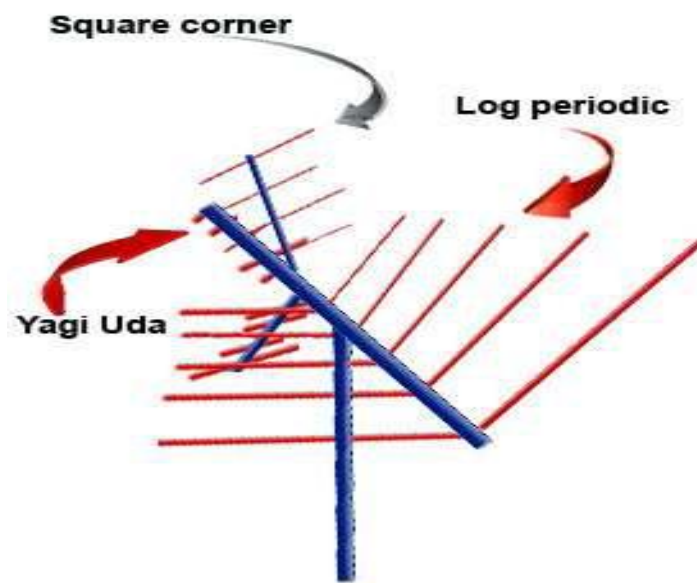


Fig 3.2m: YUCOLP (Yagi-Uda-Corner-Log-Periodic) hybrid array

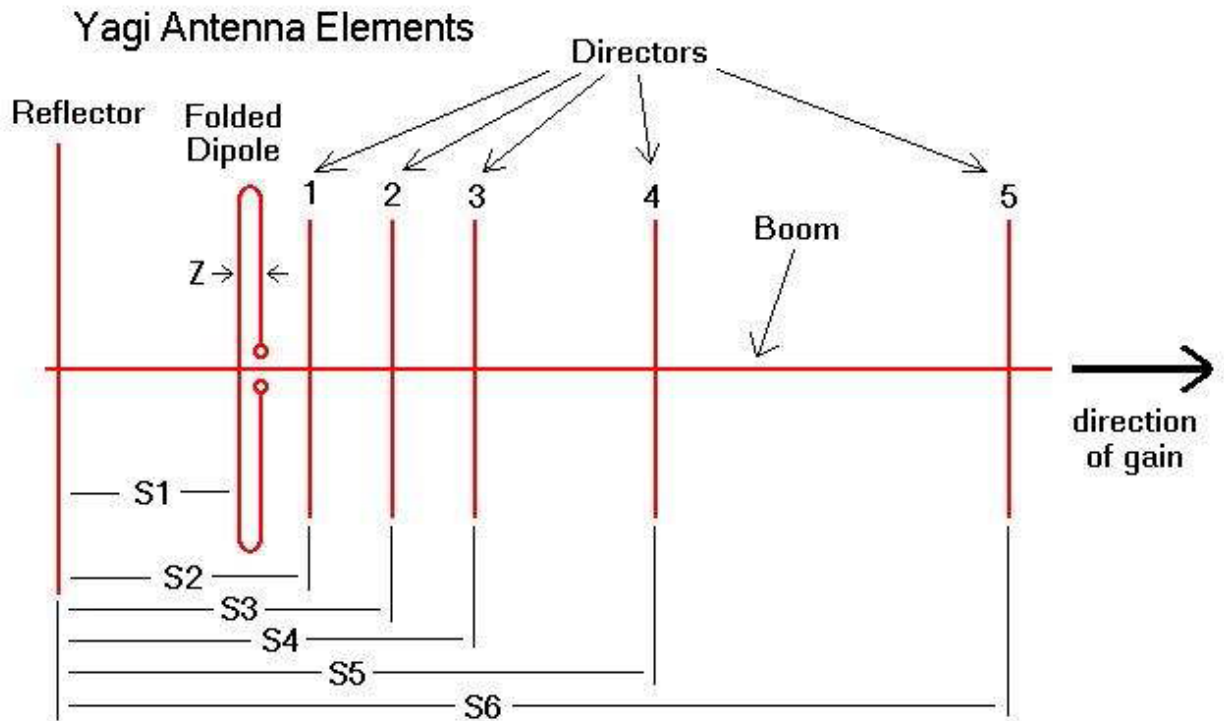


Fig 3.2n: Yagi antenna details

The total included angle of the V-dipoles is 120° . As frequency increases, the active region moves from the large to the small end of the LP array in the $\lambda/2$ mode, then from the large to the small end in the $3\lambda/2$ mode, next to the corner reflector and finally to the YU array. The corner-YU array provides more gain for the UHF band than possible with a high frequency extension of the LP array [10].

CHAPTER 4

FAMILIARIZATION WITH HFSS

4.1 Introduction

HFSS is a high-performance full-wave electromagnetic (EM) field simulator for arbitrary 3D volumetric passive device modeling that takes advantage of the familiar Microsoft Windows graphical user interface. It integrates simulation, visualization, solid modeling, and automation in an easy-to-learn environment where solutions to 3D EM problems are quickly and accurately obtained.

Ansoft HFSS employs the Finite Element Method (FEM), adaptive meshing, and graphics to give unparalleled performance and insight to all types of 3D EM problems. Ansoft HFSS can be used to calculate parameters such as S-Parameters, Resonant Frequency, and Fields.

Typical uses include:

Package Modeling: – BGA, QFP, Flip-Chip

PCB Board Modeling: – Power/Ground planes, Mesh Grid Grounds, Backplanes

Silicon/GaAs: - Spiral Inductors, Transformers

EMC/EMI: – Shield Enclosures, Coupling, Near- or Far-Field Radiation

Antennas/Mobile Communications: – Patches, Dipoles, Horns, Conformal Cell Phone Antennas, Quadrafilar Helix, Specific Absorption Rate(SAR), Infinite Arrays, Radar Cross Section(RCS), Frequency Selective Surfaces(FSS)

Connectors: – Coax, SFP/XFP, Backplane, Transitions

Waveguide: – Filters, Resonators, Transitions, Couplers

Filters: – Cavity Filters, Microstrip, Dielectric

4.2 Working Principle

The Ansoft HFSS Desktop provides an intuitive, easy-to-use interface for developing passive RF device models. Creating designs, involves the following:

1. Parametric Model Generation – creating the geometry, boundaries and excitations.
2. Analysis Setup – defining solution setup and frequency sweeps
3. Results – creating 2D reports and field plots
4. Solve Loop - the solution process is fully automated to understand how these processes co-exist, examine the illustration shown below.

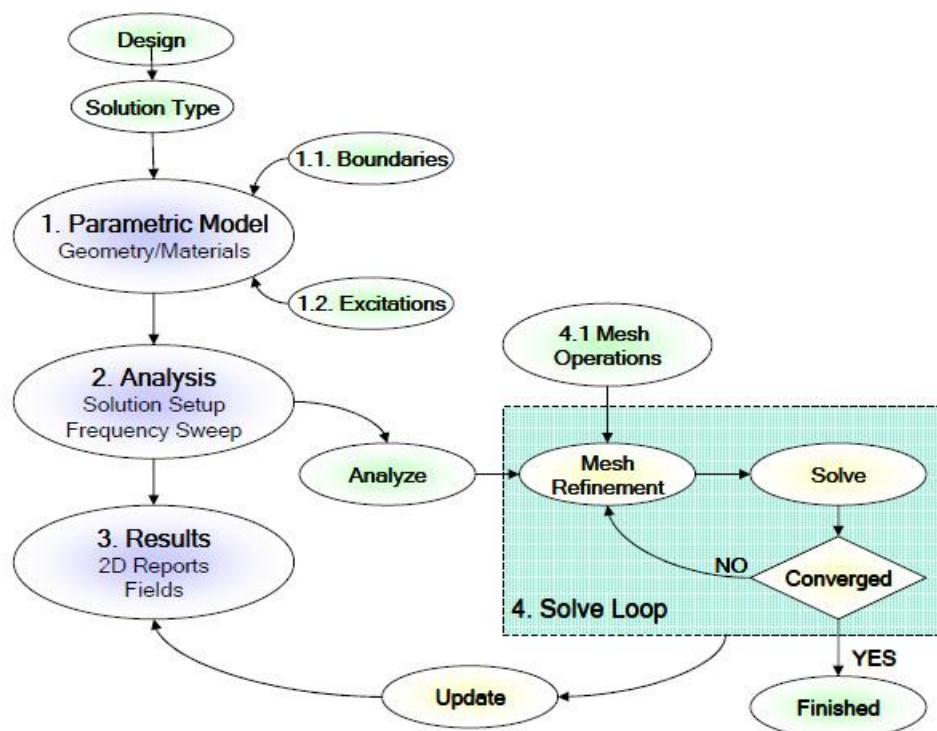


Figure 4.2: HFSS Solution Process

4.3 Boundary Conditions

Boundary conditions enable to control the characteristics of planes, faces, or interfaces between objects. Boundary conditions are important to understand and are fundamental to solution of Maxwell's equations.

There are three types of boundary conditions. The first two are largely the user's responsibility to define them or ensure that they are defined correctly. The material boundary conditions are transparent to the user.

1. Excitations

Wave Ports (External)

Lumped Ports (Internal)

2. Surface Approximations

Symmetry Planes

Perfect Electric or Magnetic Surfaces

Radiation Surfaces

Background or Outer Surface

3. Material Properties

Boundary between two dielectrics

Finite Conductivity of a conductor

4.4 Technical Definition

Excitation: An excitation port is a type of boundary condition that permits energy to flow into and out of a structure.

Perfect E: Perfect E is a perfect electrical conductor, also referred to as a perfect conductor. This type of boundary forces the electric field (E-Field) perpendicular to the surface. There are also two automatic Perfect E assignments:

Any object surface that touches the background is automatically defined to be a Perfect E boundary and given the boundary condition name outer.

Any object that is assigned the material pec (Perfect Electric Conductor) is automatically assigned the boundary condition Perfect E to its surface and given the boundary condition name smetal.

Perfect H: Perfect H is a perfect magnetic conductor. Forces E-Field tangential to the surface.

Natural: For a Perfect H boundary that overlaps with a perfect E boundary, this

reverts the selected area to its original material, erasing the Perfect E boundary condition. It does not affect any material assignments. It can be used, for example, to model a cut-out in a ground plane for a coax feed.

Finite Conductivity: A Finite Conductivity boundary enables you to define the surface of an object as a lossy (imperfect) conductor. It is an imperfect E boundary condition, and is analogous to the lossy metal material definition. To model a lossy surface, you provide loss in Siemens/meter and permeability parameters. Loss is calculated as a function of frequency. It is only valid for good conductors. Forces the tangential E-Field equal to $Z_s(n \times H_{tan})$. The surface impedance (Z_s) is equal to, $(1+j)/(\delta\sigma)$, where:

δ is the skin depth, $(2/(\omega\sigma\mu))^{0.5}$ of the conductor being modeled

ω is the frequency of the excitation wave.

σ is the conductivity of the conductor.

μ is the permeability of the conductor.

Impedance: A resistive surface that calculates the field behavior and losses using analytical formulas. Forces the tangential E-Field equal to $Z_s(n \times H_{tan})$. The surface impedance is equal to $R_s + jX_s$, where:

R_s is the resistance in ohms/square

X_s is the reactance in ohms/square

Layered Impedance: Multiple thin layers in a structure can be modeled as an impedance surface. See the Online Help for additional information on how to use the Layered Impedance boundary.

Lumped RLC: A parallel combination of lumped resistor, inductor, and/or capacitor surface. The simulation is similar to the Impedance boundary, but the software calculates the ohms/square using the user supplied R, L, C values.

Infinite Ground Plane: Generally, the ground plane is treated as an infinite, Perfect E, Finite Conductivity, or Impedance boundary condition. If radiation boundaries are used in a structure, the ground plane acts as a shield for far-field energy, preventing waves from propagating past the ground plane. To simulate the effect of an infinite ground plane, check the Infinite ground plane box when defining a Perfect E, Finite Conductivity, or Impedance boundary condition.

Radiation: Radiation boundaries, also referred to as absorbing boundaries, enable you to model a surface as electrically open: waves can then radiate out of the structure and toward the radiation boundary. The system absorbs the

wave at the radiation boundary, essentially ballooning the boundary infinitely far away from the structure and into space. Radiation boundaries may also be placed relatively close to a structure and can be arbitrarily shaped. This condition eliminates the need for a spherical boundary. For structures that include radiation boundaries, calculated S-parameters include the effects of radiation loss. When a radiation boundary is included in a structure, far-field calculations are performed as part of the simulation.

CHAPTER 5

DESIGN OF LPDA

5.1 Introduction

Compact, very low-cost printed antennas with both wideband and Omni-directional characteristics are desired in modern communications systems. Dipole antennas have been popular candidates in many systems for their uniform Omni-directional coverage, reasonable gain, and relatively low manufacturing cost. Despite the advantages mentioned above, dipole antennas suffer from relatively narrow bandwidth, about 10% for $VSWR < 2:1$. This bandwidth problem has limited their application in modern multi-band communication systems. In addition, nearby objects easily detune the dipoles because of the limited bandwidth of operation [15].

In modern telecommunication systems, antennas with wider bandwidth and smaller dimensions than conventional ones are preferred. Log-Periodic antennas are designed for the specific purpose of having a very wide bandwidth. The achievable bandwidth is theoretically infinite; the actual bandwidth achieved is dependent on how large the structure is (to determine the lower frequency limit) and how precise the finer (smaller) features are on the antenna (which determines the upper frequency limit) [16].

In telecommunication, a log-periodic antenna (LP, also known as a log-periodic array or log periodic beam antenna/aerial) is a broadband, multi-element, directional, narrow-beam antenna that has impedance and radiation characteristics that are regularly repetitive as a logarithmic function of the excitation frequency. The individual components are often dipoles, as in a log-periodic dipole array (LPDA). Log-periodic antennas are designed to be self-similar and are thus also fractal antenna arrays [17]. Increasing number of log periodic fractal iteration reduces return loss, especially in higher frequencies, however, increases the antenna bandwidth [18]. The log periodic antenna is used in a number of applications where a wide bandwidth is required along with directivity and a modest level of gain. It is sometimes used on the HF portion of the spectrum where operation is required on a number of frequencies to enable communication to be maintained. It is also used at VHF and UHF for a variety of applications, including some uses as a television antenna.

The lengths and spacing of the elements of a log-periodic antenna increase logarithmically from one end to the other. This antenna design is used where a wide range of frequencies is needed while still having moderate gain and directionality [17].

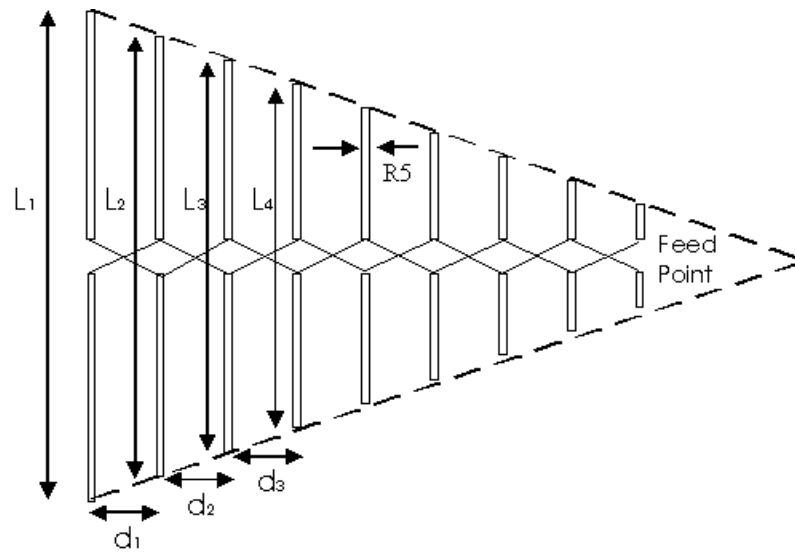


Figure 5.1: Schematic diagram of log-periodic dipole antenna

The successive dipoles are connected alternately to a balanced transmission line called feeder. That is to say these closely spaced elements are oppositely connected so that entire radiation in the direction of the shorter elements is created and broadside radiation tends to cancel. Actually, a coaxial line running through one of the feeders from the longest element to the shortest is used. The center conductor of the coaxial cable is connected to the other feeder so that the antenna has its own balun [19].

Radiation energy, at a given frequency, travels along the feeder until it reaches a section of the structure where the electrical lengths of the elements and phase relationships are such as to produce the radiation. As frequency is varied, the position of the resonant element is moved smoothly from one element to the next. The upper and lower frequency limits will then be determined by lengths of the shortest and longest elements or conversely these lengths must be chosen to satisfy the bandwidth requirement. The longest half-element must be roughly $\frac{1}{4}$ wavelength at the lowest frequency of the bandwidth, while the shortest half element must be about $\frac{1}{4}$ wavelength at the highest frequency in the desired operating bandwidth [20].

It is possible to explain the operation of a log periodic array in straightforward terms. The feeder polarity is reversed between successive elements. Take the condition when this RF antenna is approximately in the middle of its operating range. When the signal meets the first few elements it will be found that they are spaced quite close together in terms of the operating wavelength. This means that the fields from these elements will cancel one another out as the feeder sense is reversed between the elements. Then as the signal progresses down the antenna a point is reached where the feeder reversal and the

distance between the elements gives a total phase shift of about 360 degrees. At this point the effect which is seen is that of two phased dipoles. The region in which this occurs is called the active region of the RF antenna. In reality the active region can consist of more elements. The actual number depends upon the angle α and a design constant. The elements outside the active region receive little direct power. Despite this it is found that the larger elements are resonant below the operational frequency and appear inductive. Those in front resonate above the operational frequency and are capacitive. These are exactly the same criteria that are found in the Yagi. Accordingly the element immediately behind the active region acts as a reflector and those in front act as directors. This means that the direction of maximum radiation is towards the feed point [21].

5.2 Design Specifications

For our desired design,

Gain, $G = 9\text{dbi}$

Lowest frequency, $f_1 = 1350\text{MHz}$

Highest frequency, $f_2 = 2690\text{MHz}$

So Upper to lower frequency ratio = 2:1

The geometrical dimensions of the log-periodic antenna follow some pattern and condition [22]. For analysis, the following notation is used:

L_n = the length of element n , and $n = 1, 2, \dots, N$;

S_n = the spacing between elements n and $(n + 1)$;

d_n = the diameter of element n ;

g_n = the gap between the poles of element n

They are related to the scaling factor:

$$\tau = \frac{L_2}{L_1} = \frac{L_{n+1}}{L_n} = \frac{S_{n+1}}{S_n} = \frac{d_{n+1}}{d_n} = \frac{g_{n+1}}{g_n} < 1 \quad (5.1)$$

and the spacing factor:

$$\sigma = \frac{S_1}{2L_1} = \frac{S_n}{2L_n} < 1 \quad (5.2)$$

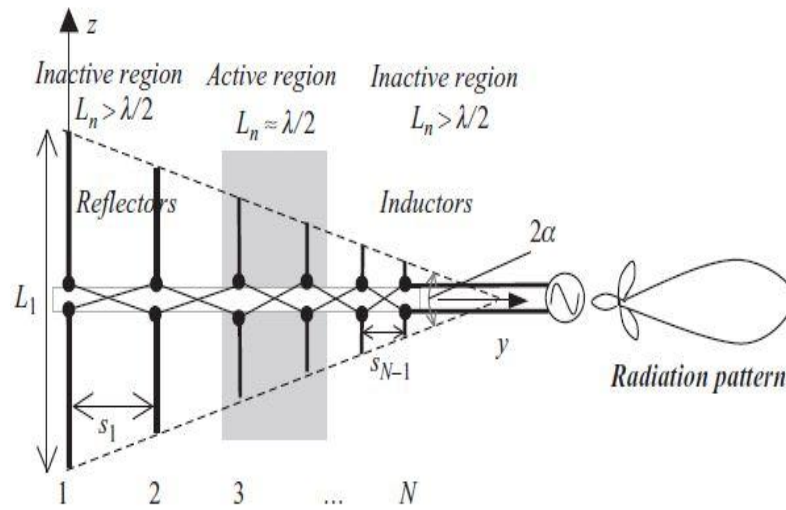


Figure 5.2a: The configuration of a log-periodic antenna and its radiation pattern [22]

As shown in Figure 5.2a, two straight lines through the dipole ends form an angle 2α , which is a characteristic of the frequency-independent structure.

The angle α is called the apex angle of the log-periodic antenna, which is a key design parameter and can be found as,

$$\tan^{-1} \frac{L_n - L_{n+1}}{2S_n} = \tan^{-1} \frac{L_n(1-\tau)}{2S_n} = \tan^{-1} \frac{(1-\tau)}{4\sigma} \quad (5.3)$$

These relations hold true for any n . From the operational principle of the antenna and the frequency point of view, Equation 5.1 corresponds to:

$$\tau = \frac{L_{n+1}}{L_n} = \frac{f_n}{f_{n+1}} \quad (5.4)$$

In practice, the most likely scenario is that the frequency range is given from f_{\min} to f_{\max} ; the following equations may be employed for design:

$$L_1 \geq \frac{\lambda_{\max}}{2} = \frac{c}{f_{\min}} \quad (5.5)$$

$$L_N \geq \frac{\lambda_{min}}{2} = \frac{c}{f_{max}} \quad (5.6)$$

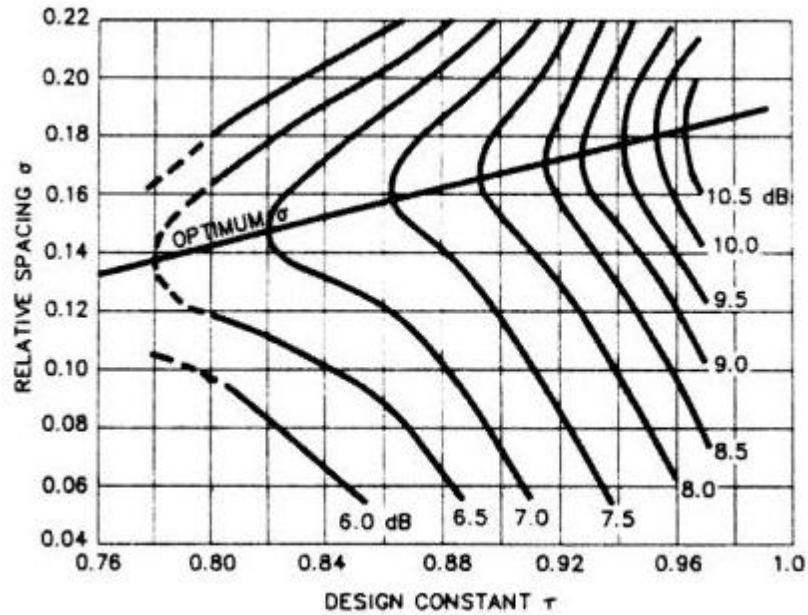


Figure 5.2b: Computed contours of constant directivity versus σ and τ for log-periodic dipole arrays.[23]

From above graph we get,

Design constant, $\tau = 0.93$

Relative spacing, $\sigma = 0.16$

Apex angle = α

Number of elements = N

5.3 Design Calculation

Design constant, $\tau = 0.93$

Relative spacing, $\sigma = 0.16$

Apex angle, α :

$$\begin{aligned}\cot \alpha &= \frac{4\alpha}{1-\tau} \\ &= \frac{4 \times 0.93}{1-0.16} \\ &= 9.14\end{aligned}$$

$$\begin{aligned}\text{So, } \tan \alpha &= \frac{1}{9.14} \\ &= 0.11\end{aligned}$$

$$\begin{aligned}\text{So } \alpha &= \tan^{-1}(0.11) \\ &= 6.3^\circ\end{aligned}$$

Number of elements:

$$N = (\log (f_1/f_2)/\log (\tau)) + 1$$

$$\text{Or, } N = (\log(1350/2960)/\log(0.93)) + 1$$

$$\text{So, } N = 10.49 \approx 11$$

To be on the safe side we should use twelve elements to make sure that the desired directivity will be achieved.

Let, $N=12$

So, we can afford to start from, say, $f'_1 = 1340$ MHz

$$L_1 = c/f'_1 = 300/1340 = 0.224 \text{ m} = 8.82 \text{ inches} \quad [1 \text{ m} = 39.37 \text{ inches}]$$

And, say, $f'_2 = 2700$ MHz

$$L_n = c/f'_2 = 300/2700 = 0.11 \text{ m} = 4.41 \text{ inches}$$

$$L_2 = L_1 \tau = (8.82)(0.93) = 8.2 \text{ inches}$$

$$L_3 = L_2 \tau = (8.2)(0.93) = 7.626 \text{ inches}$$

$$L_4 = L_3 \tau = (7.626)(0.93) = 7.09 \text{ inches}$$

$$L_5 = L_4 \tau = (7.09)(0.93) = 6.59 \text{ inches}$$

$$L_6 = L_5 \tau = (6.59)(0.93) = 6.128 \text{ inches}$$

$$L_7 = L_6 \tau = (6.128)(0.93) = 5.69 \text{ inches}$$

$$L_8 = L_7 \tau = (5.69)(0.93) = 5.3 \text{ inches}$$

$$L_9 = L_8 \tau = (5.3)(0.93) = 4.93 \text{ inches}$$

$$L_{10} = L_9 \tau = (4.93)(0.93) = 4.58 \text{ inches}$$

$$L_{11} = L_{10} \tau = (4.58)(0.93) = 4.26 \text{ inches}$$

$$L_{12} = L_{11} \tau = (4.26)(0.93) = 3.96 \text{ inches}$$

$$\text{Now, } S_n = 2(L_n \tau)$$

$$S_1 = 2(8.82)(0.16) = 2.82$$

$$S_2 = 2(8.2)(0.16) = 2.62$$

$$S_3 = 2(7.626)(0.16) = 2.44$$

$$S_4 = 2(7.09)(0.16) = 2.27$$

$$S_5 = 2(6.59)(0.16) = 2.108$$

$$S_6 = 2(6.128)(0.16) = 1.96$$

$$S_7 = 2(5.69)(0.16) = 1.82$$

$$S_8 = 2(5.3)(0.16) = 1.696$$

$$S_9 = 2(4.93)(0.16) = 1.577$$

$$S_{10} = 2(4.58)(0.16) = 1.466$$

$$S_{11} = 2(4.26)(0.16) = 1.363$$

$$S_{12} = 2(3.96)(0.16) = 1.267$$

So, total length of the antenna,

$$L = S_1 + S_2 + S_3 + S_4 + S_5 + S_6 + S_7 + S_8 + S_9 + S_{10} + S_{11} + S_{12}$$

$$= 23.4072 \text{ inches}$$

$$= 1.95 \text{ Ft}$$

Table-1: Measurement of Designed Antenna Elements

Element No.	Spacing(inch)	Length(inch)
1	2.82	$(8.82/2)=4.41$
2	2.62	$(8.2/2)=4.1$
3	2.44	$(7.626/2)=3.813$
4	2.27	$(7.09/2)=3.545$
5	2.108	$(6.59/2)=3.295$
6	1.96	$(6.128/20)=3.064$
7	1.82	$(5.69/2)=2.845$
8	1.696	$(5.3/2)=2.65$
9	1.577	$(4.93/2)=2.465$
10	1.466	$(4.58/2)=2.29$
11	1.363	$(4.26/2)=2.16$
12	1.267	$(3.96/2)=1.98$

Chapter 6

PERFORMANCE ANALYSIS

6.1 Design Structure & Simulation Results

Design structure:

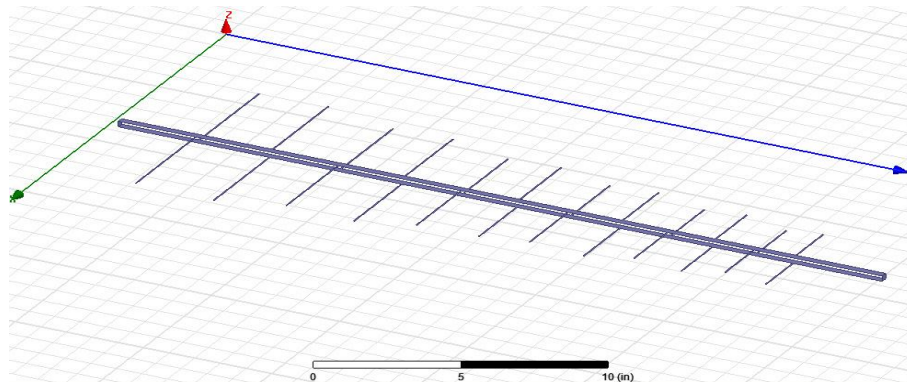


Figure 6.1a: LPDA antenna design structure in HFSS Simulation

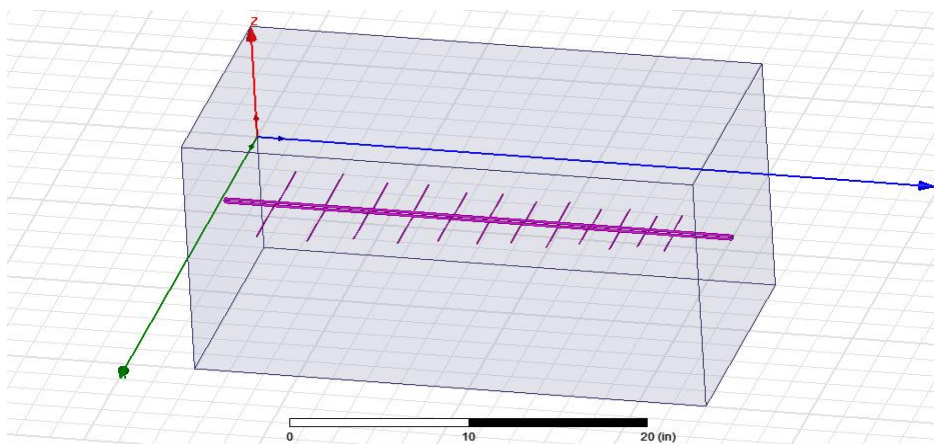


Figure 6.1b: LPDA antenna design structure for simulation with radiation box

In the figure 6.1a designed LPDA antenna is shown without radiation box in HFSS window.

In the figure 6.1b designed LPDA antenna is shown with radiation box in HFSS window.

Simulation Result:

Return Loss Characteristic (frequency vs. dB(S(1,1)) curve) :

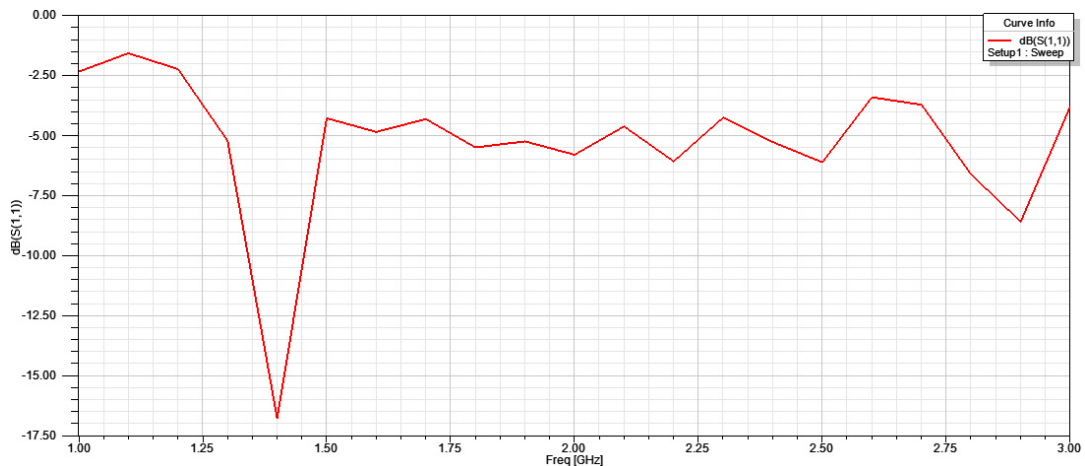


Figure 6.1c: Frequency vs. dB(S(1,1)) curve when simulated between 1-3 GHz

One of the most commonly used parameters in regards to antennas is S(1,1). S(1,1) represents how much power is reflected from antenna and hence is known as reflection coefficient or return loss.

If, $S(1,1) = 0$ db, then all power is reflected from the antenna and nothing is radiated. If, $S(1,1) = -8$ db, this implies that if 3 db of power is delivered to the antenna, -5 db is the reflected power. The remainder of power is “accepted by” or “delivered to” the antenna. This accepted power is either radiated or absorbed as losses within the antenna. Since antennas are typically designed to be low loss, the majority of power delivered to the antenna, is radiated.

The above figure implies that the antenna radiates best at 1.35 GHz where $S(1,1) = -17$ db. Further at 1.25 GHz the antenna will radiate virtually nothing as $S(1,1)$ is close to 0 db.

The antenna bandwidth can also be determined from above figure. If the bandwidth is defined as the frequency range where $S(1,1)$ is to be less than -

3db ,then the bandwidth would be roughly 1.3 GHz with 2.65 the higher end and 1.35 the lower end of the frequency band.

The 3D curve of return loss characteristic is also shown below:

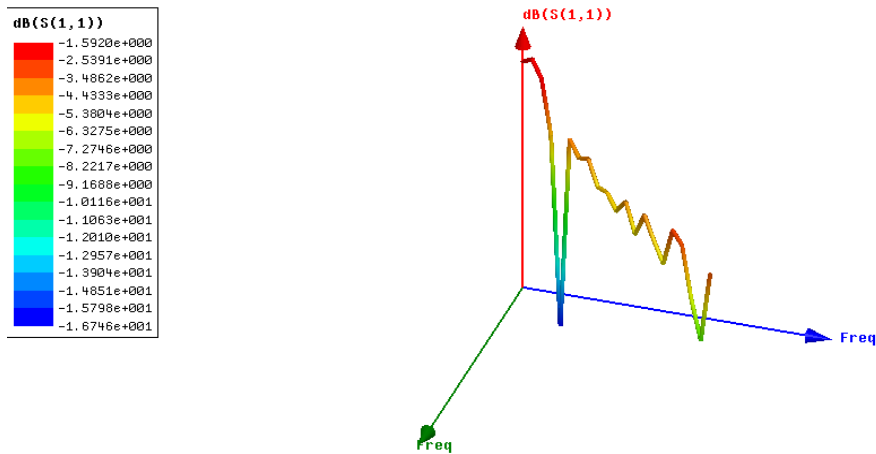


Figure 6.1d: 3-D rectangular plot of Frequency vs. $dB(S(1,1))$ when simulated between 1-3 GHz

Frequency vs. VSWR:

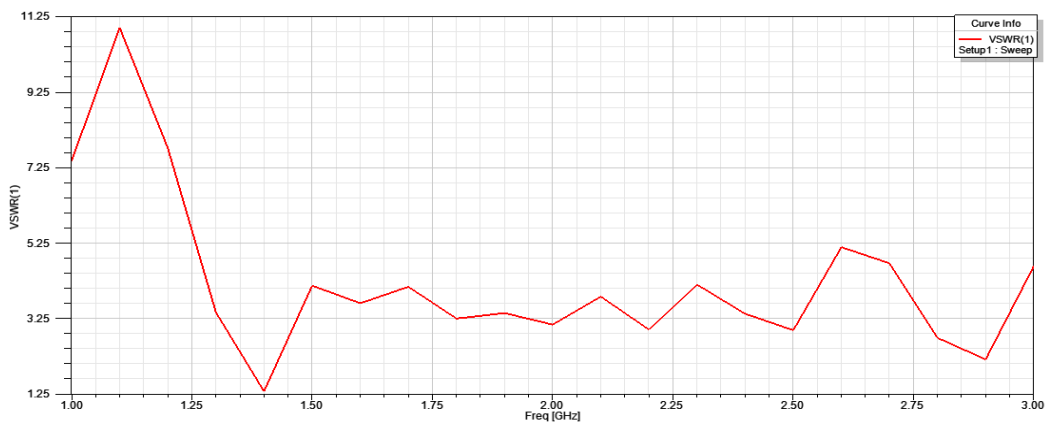


Figure 6.1e: Frequency vs. VSWR curve

VSWR, i.e, voltage standing wave ratio, is a function of reflection coefficient, Γ , which describes the power reflected from the antenna. The relation between reflection coefficient and VSWR can be shown by the following formula

$$VSWR = \frac{1+\Gamma}{1-\Gamma}$$

VSWR is always a real and positive number for antennas. It is clear that, the smaller VSWR, hence reflection coefficient, the better the antenna is matched to transmission line and more power is delivered to the antenna. The minimum VSWR is 1.0, which means no power is reflected from the antenna, is the ideal condition.

VSWR is measure of how much power is delivered to an antenna. This doesn't mean that antenna radiates all the power it receives. So VSWR measures the potential to radiate. A low VSWR means antenna is well matched but doesn't necessarily mean the power delivered is also radiated.

In the above figure VSWR is less than 4. This implies that VSWR is less than 4 over the specified frequency range (in our case 1400 MHz – 2600 MHz). This VSWR specification also implies that the reflection coefficient is less than 0.5 over the specified frequency range.

The 3D rectangular curve of frequency vs. VSWR is also shown below:

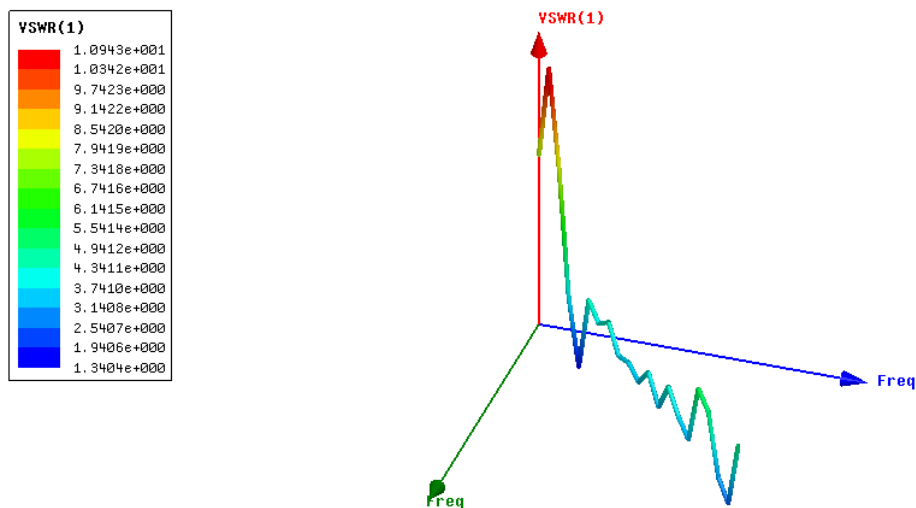


Figure 6.1f: 3-D rectangular plot of Frequency vs. VSWR when simulated between 1-3 GHz

Gain Vs Directivity:

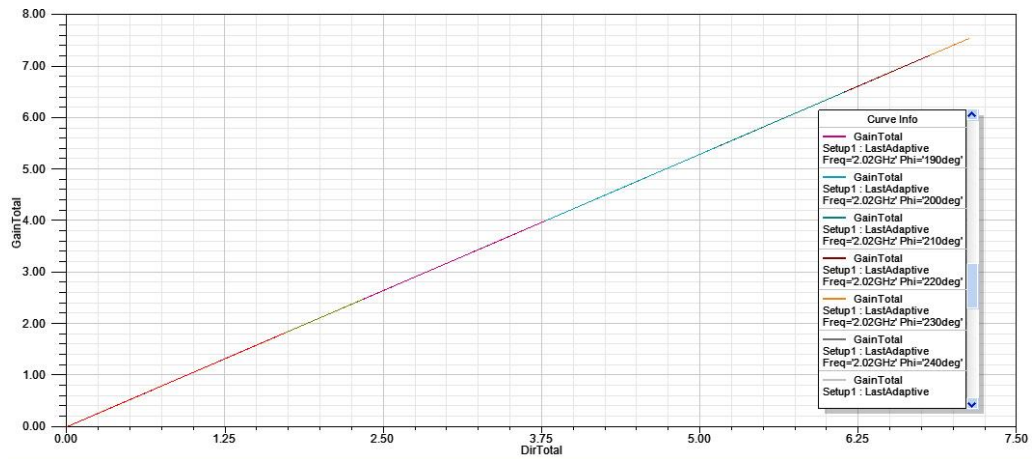


Figure 6.1g: Gain Vs Directivity Curve

The relation of gain and directivity is $G = \epsilon_r D$ which is similar to the straight line equation $y = mx$. So the plot must be a straight line.

From the above figure we can see that the gain vs directivity curve curve is a straight line along the origin.

Total Gain vs theta (deg):

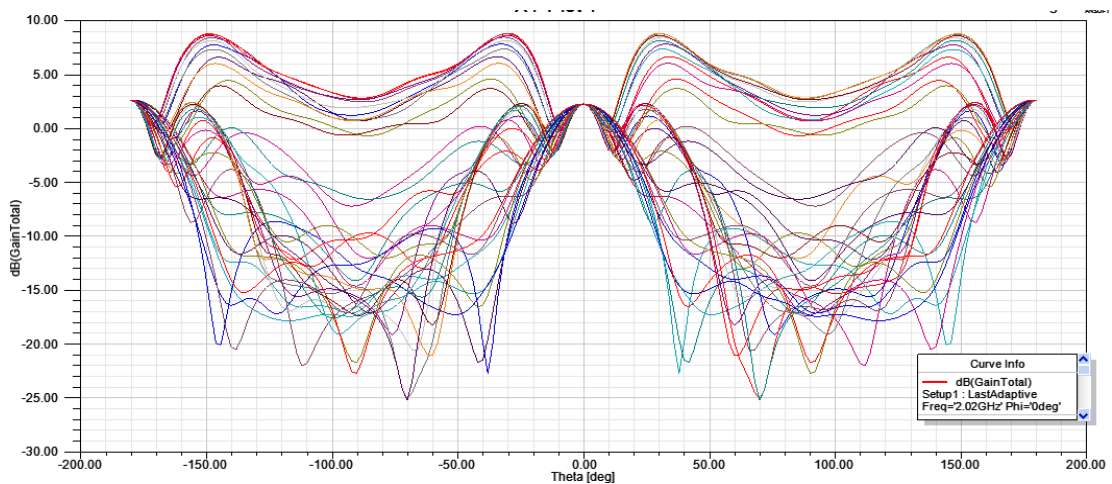


Figure 6.1h:Gain(dB) vs theta (deg) Curve

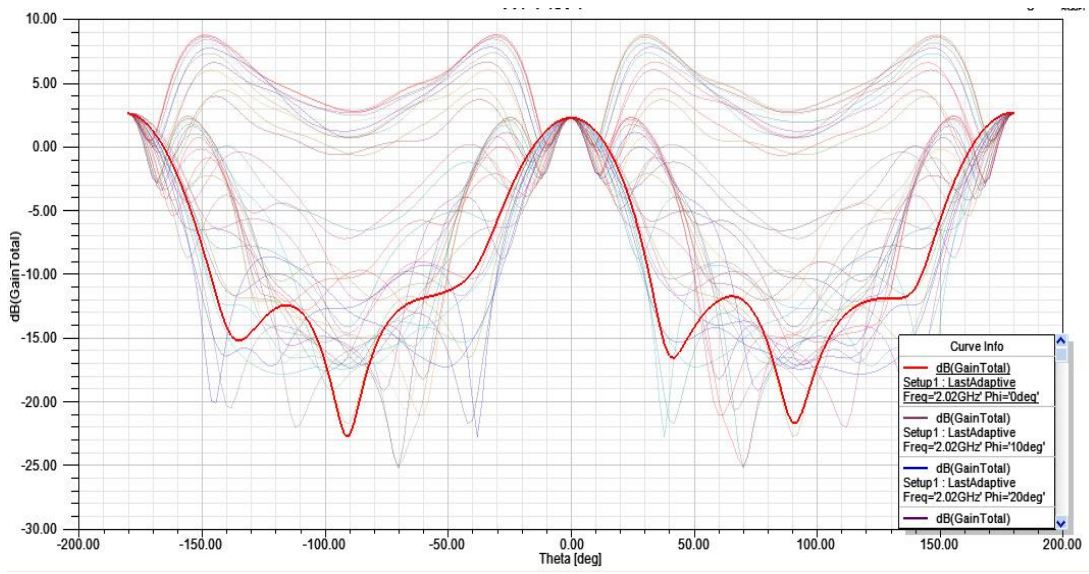


Figure 6.1i: Total Gain(db) vs theta (deg) curve at frequency=2.02GHz, phi=0 deg

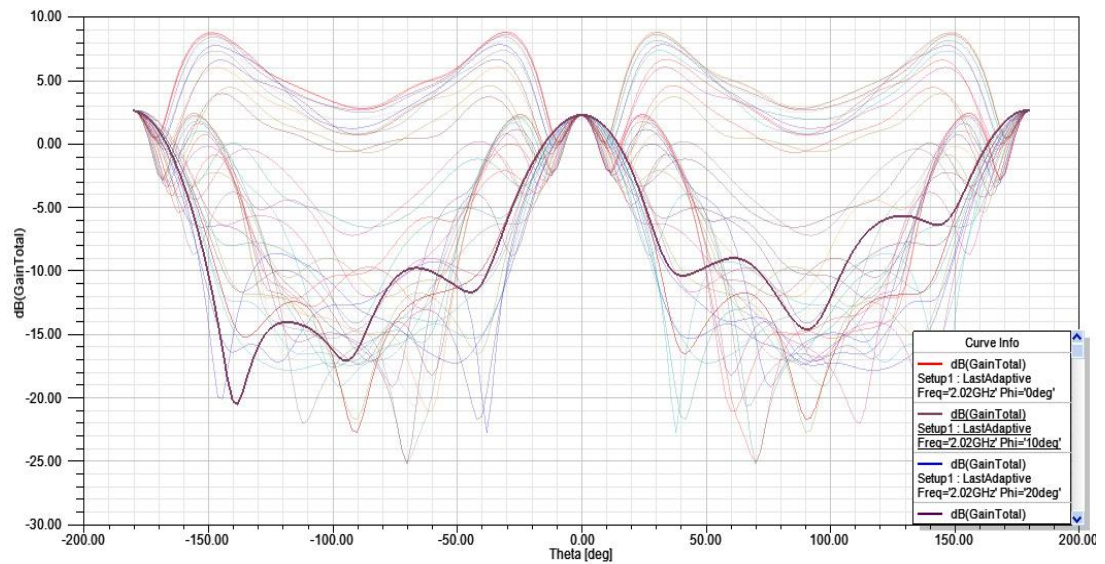


Figure 6.1j: Total Gain(db) vs theta (deg) curve at frequency=2.02GHz, phi = 10 deg

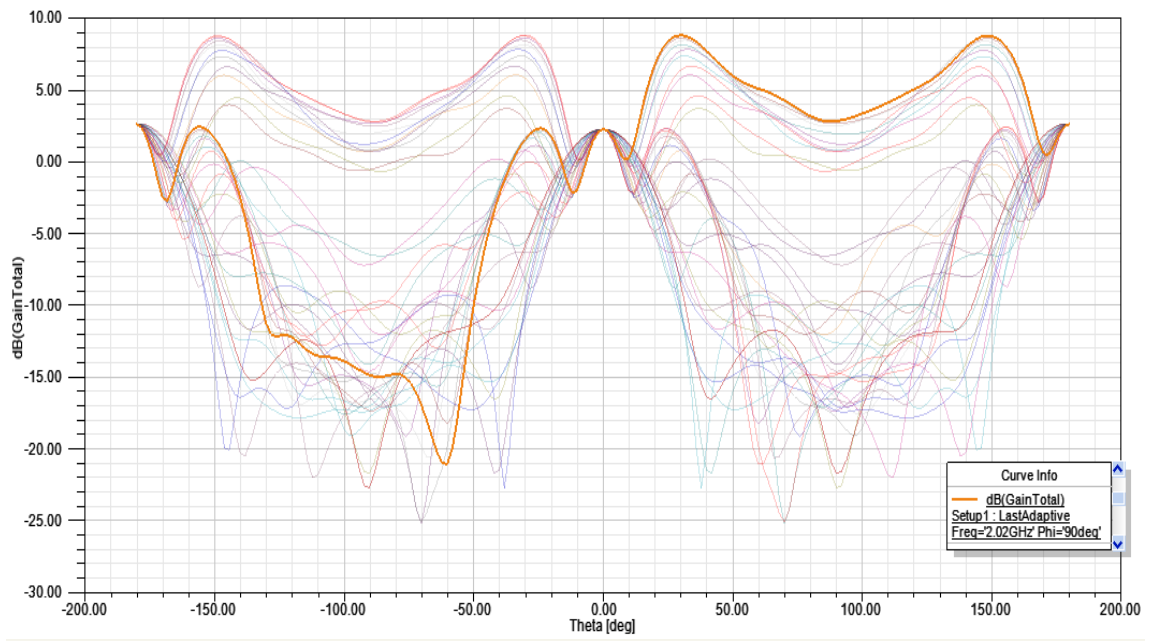


Figure 6.1k: Total Gain(db) vs theta (deg) curve at frequency=2.02GHz, phi=90 deg

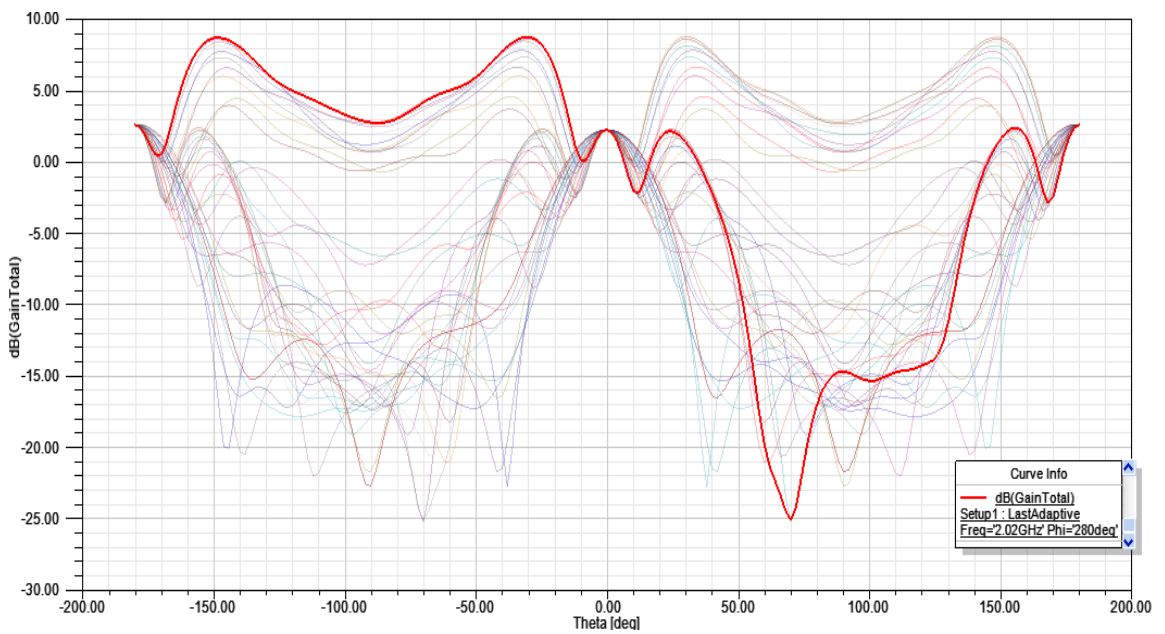


Figure 6.1l: Total Gain(db) vs theta (deg) curve at frequency=2.02GHz, phi=280 deg

The solution frequency needed to run the analysis is 2.02 GHz which is also the center frequency between the start and stop point. So all the solutions are given in the solution frequency.

Figure 6.1h shows the total gain(db) curve for all values of phi (0° - 360°).

From the curve we can see that the expected dbi gain which is 9dbi has almost achieved.

Figure 6.1k shows the maximum gain(db) = 8.7 dbi at phi = 90° while figure 6.1l shows the max gain(db) = 8.7 dbi at phi = 280°.

6.2 Radiation Pattern

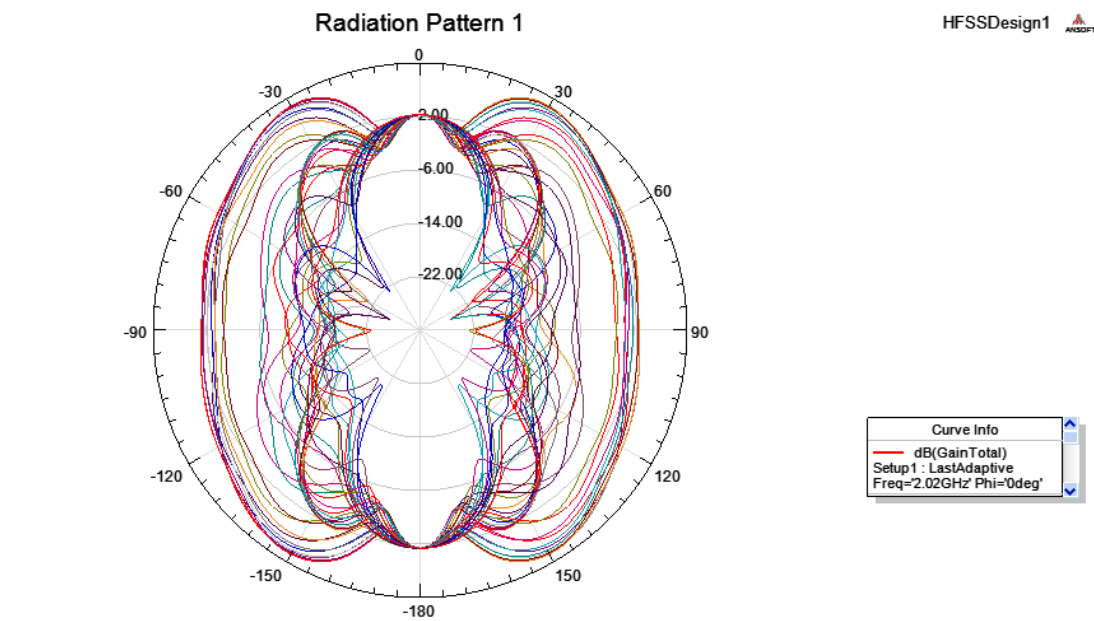


Figure 6.2a: Total Radiation pattern

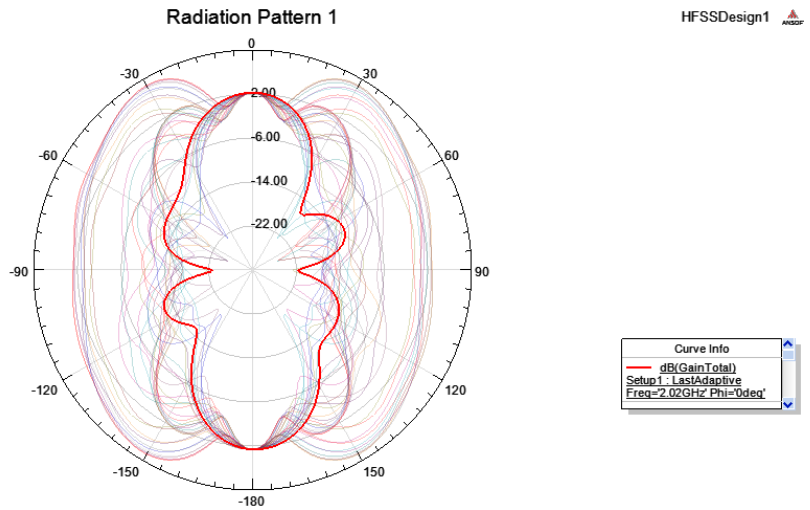


Figure 6.2b: Radiation Pattern at frequency =2.02GHz, phi=0 deg

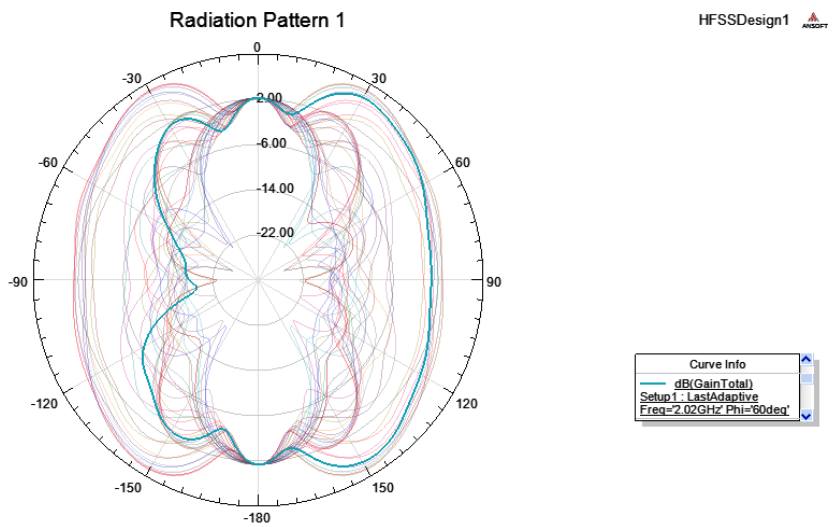


Figure 6.2c: Radiation Pattern at frequency =2.02GHz, phi=60 deg

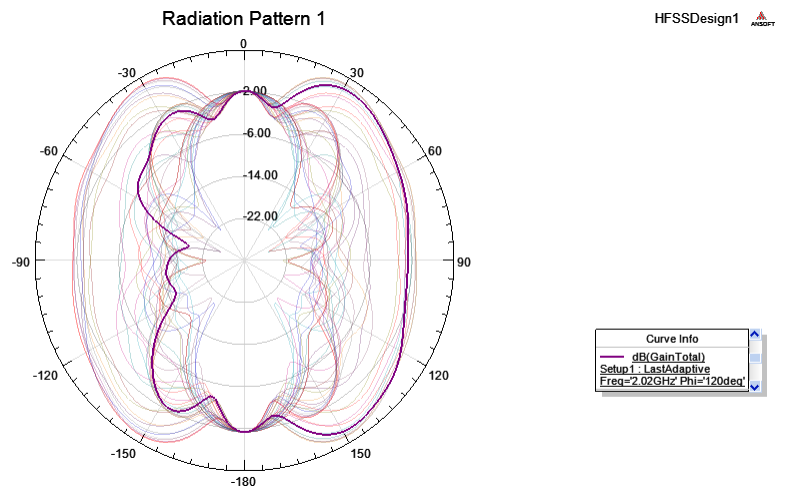


Figure 6.2d: Radiation Pattern at frequency =2.02GHz, phi=120 deg

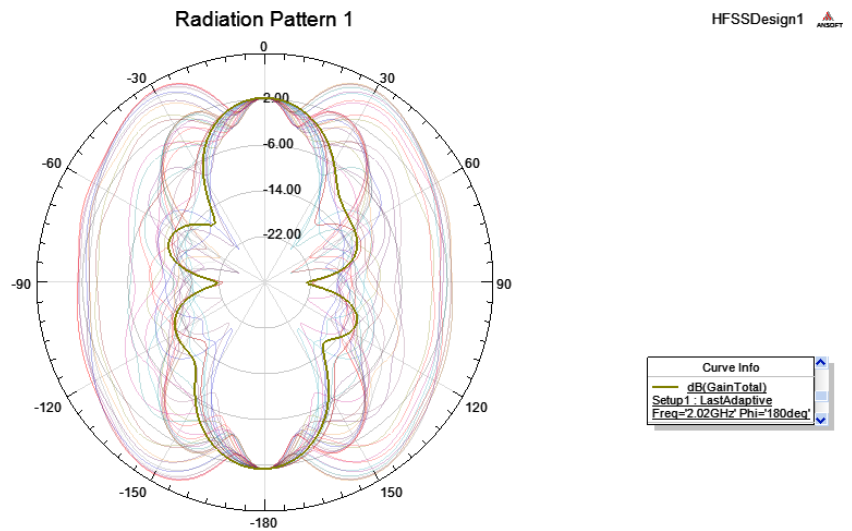


Figure 6.2e: Radiation Pattern at frequency = 2.02 GHz, phi= 180 deg

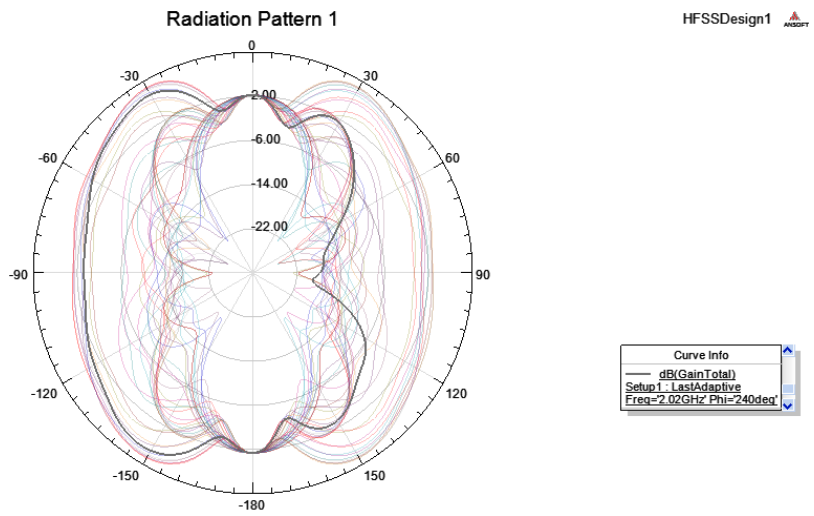


Figure 6.2f: Radiation Pattern at frequency = 2.02 GHz, phi= 240 deg

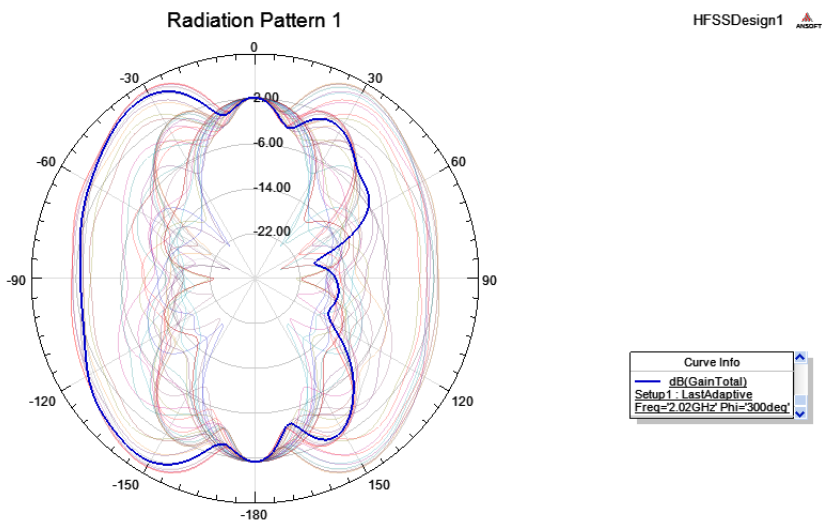


Figure 6.2g: Radiation Pattern at frequency = 2.02 GHz, phi= 300 deg

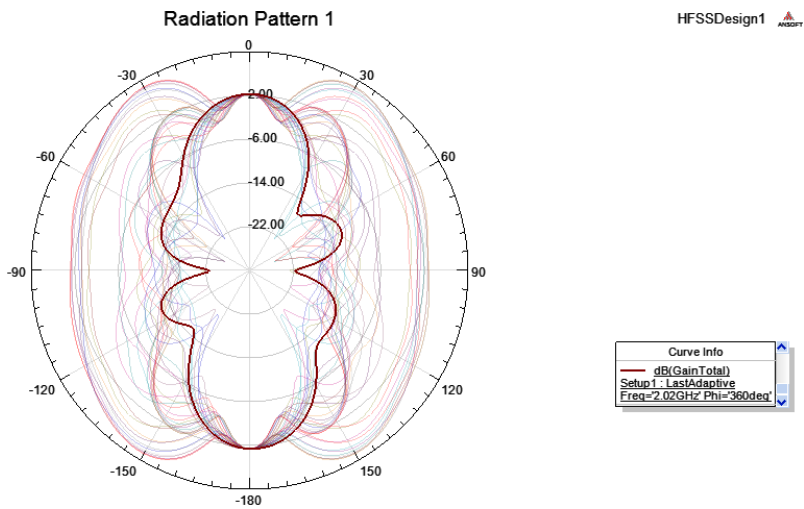


Figure 6.2h: Radiation Pattern at frequency = 2.02 GHz, phi= 360 deg

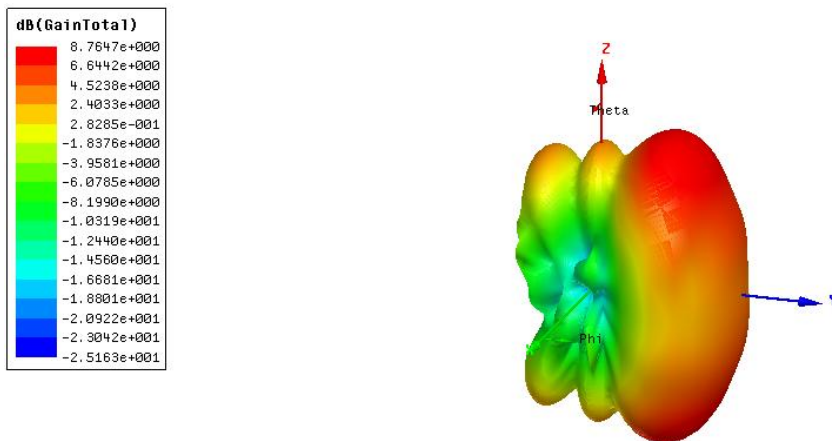


Figure 6.2i: 3-D Radiation pattern of designed LPDA

6.3 Current Density on the Surface

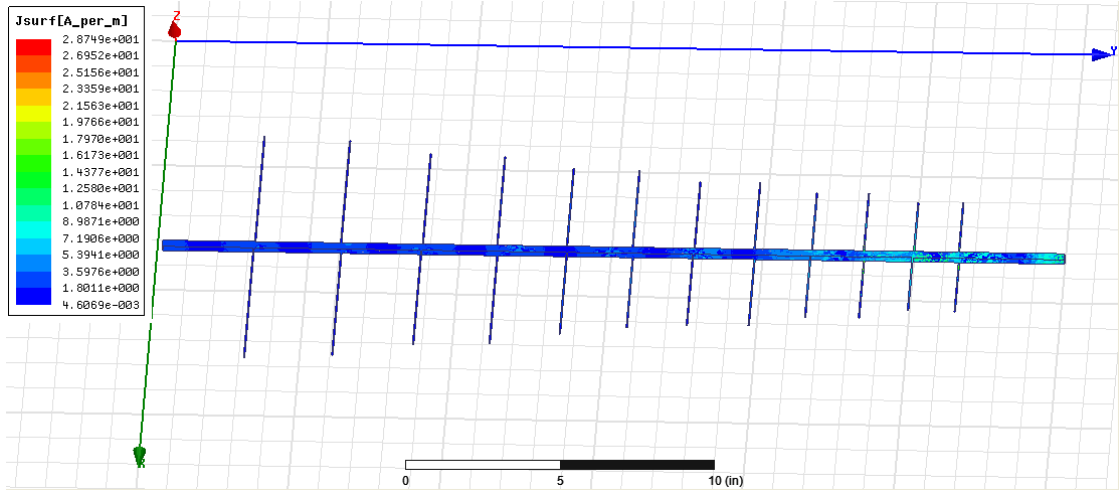


Figure 6.3a: Current density at 1GHz

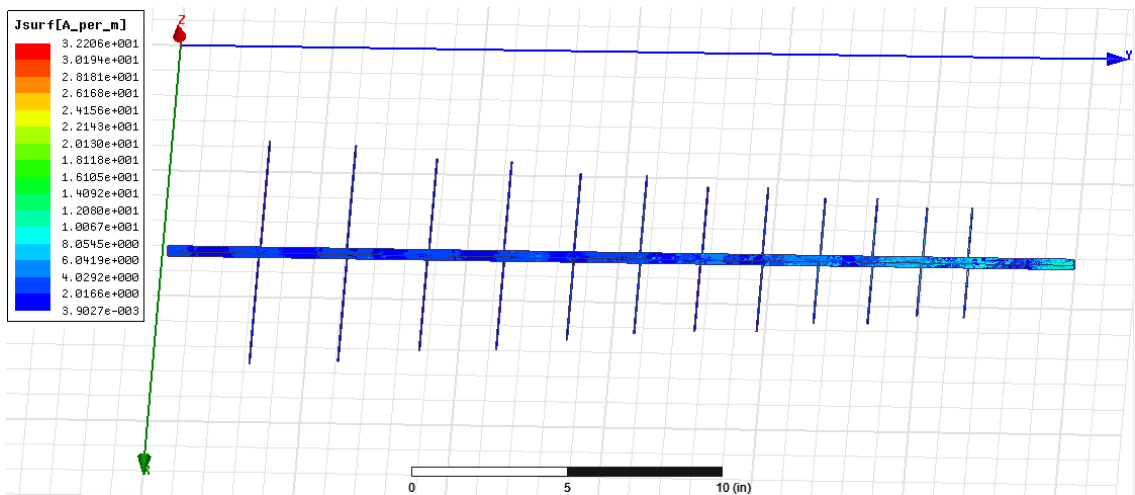


Figure 6.3b: Current density at 1.5 GHz

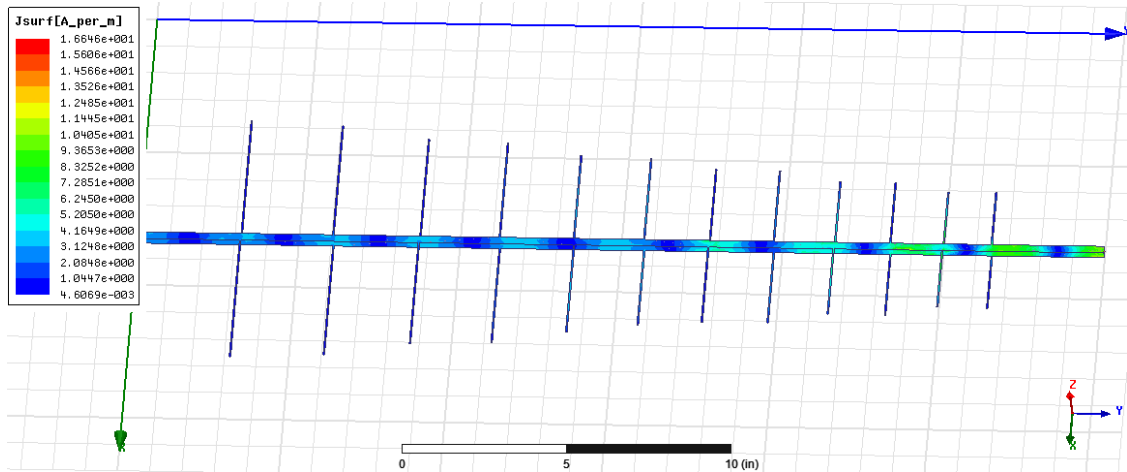


Figure 6.3c: Current density at 2.02 GHz

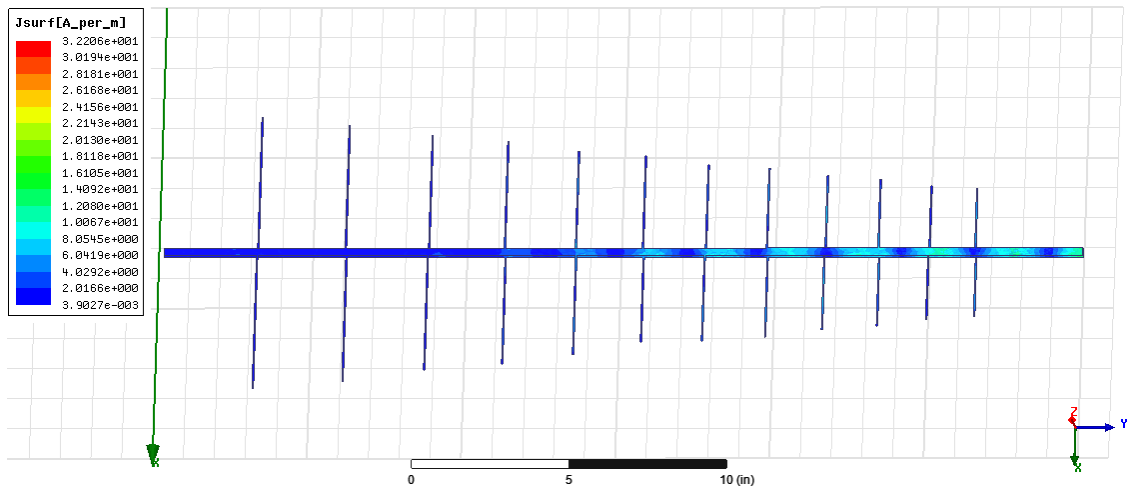


Figure 6.3d: Current density at 2.5 GHz

In the current density figure, at lower frequencies current flows in larger elements where as at higher frequencies the smaller elements are active.

In our figure (simulated by HFSS), different current densities in different elements of the antenna are indicated by different colors. Blue color has low current density (from 4.6×10^{-3} A/m to 5.39 A/m), while green colors have medium current density (from 8.9 A/m to 11 A/m) and red colors have high current density (from 25 A/m to 29 A/m).

From figure 6.3a for 1 GHz, we can see that larger elements have low current densities which are indicated by pure blue color(4.6069×10^{-3} A/m), and smaller elements have higher density than the larger elements which are indicated by light green colors (10.754 A/m).

From figure 6.3b for 1.5 GHz, we can see that larger elements have low current densities which are indicated by pure blue color (3.9×10^{-3} A/m) and smaller elements have higher density than the larger elements which are indicated by light green colors(10.1 A/m)

From figure 6.3c for 2.02 GHz, we can see that larger elements have low current densities which are indicated by light blue color(3.12 A/m) and smaller elements have higher density than the larger elements which are indicated by pure green colors(11.4 A/m).

From fig 6.3d for 2.50 GHz, we can see that larger elements have low current densities which are indicated by light blue color(8.05 A/m) and smaller elements have higher density than the larger elements which are indicated by pure green colors(18.1 A/m).

6.4 Output Parameters Calculation

The simulated result of the log periodic dipole antenna that we got from the HFSS simulator is shown in the following table –

Table 2: List of output antenna parameters

Quantity	Value
Max U	0.405905(W/sr)
Peak Directivity	7.11868
Peak Gain	$7.5243 = 10\log(7.5243) = 8.76$ dbi
Peak Realized Gain	5.10088
Radiated Power	0.716548(W)
Accepted Power	0.677921(W)
Incident Power	1(W)
Radiation Efficiency	1.05698
Front to Back Ratio	5.09764
Decay Factor	0

In the HFSS simulator we set the incident power as 1W.

From the Table we can see that our resultant maximum intensity is 0.405905 W/sr.

$$\text{This is because } U = \frac{1}{2} \frac{|\vec{E}|^2}{n_0} r^2$$

Where , n_0 = intrinsic impedance for free space = 376.7 ohms

$$r|\vec{E}| = 17.4944 \text{ V}$$

So, $U = 0.406 \text{ W/sr}$

$$\text{Peak Directivity} = 4\pi \frac{U_{\max}}{P_{\text{rad}}} = 7.118$$

$$\text{Again, Peak Gain} = 4\pi \frac{U_{\max}}{P_{\text{acceptance}}} = 7.5243$$

$$= 10\log(7.5243)$$

$$= 8.76 \text{ dbi}$$

Which is tends to our desired gain 9dbi.

$$\text{Peak Realized Gain} = 4\pi \frac{U_{\max}}{P_{\text{incident}}} = 5.100$$

We have got the radiated power = 0.716548(W) and accepted power = 0.677921(W).

$$\text{So Radiation Efficiency} = \frac{\text{Radiated Power}}{\text{Accepted Power}} = 1.05698$$

The radiation efficiency is more than 1 because our structure was assumed lossless. Therefore, the dielectric loss tangent set to zero and no conductive value for conducting materials was chosen. The antenna elements were considered perfect conductors during analysis. This above setting is enough to obtain 100% efficiency.

Before reaching the final value HFSS does millions of calculation of long decimal numbers during one simulation and takes a round off value as a final value. So many round offs could reach a final value a little over exact value. So true efficiency is 100% but because of the round off calculation process of HFSS it became a little over the exact value.

Front to back ratio is simply a ratio of the signal level in the forward direction to the reverse direction. This is normally expressed in db.

$$\text{Front to back ration} = \frac{\text{Signal in foreard direction}}{\text{Signal in reverse direction}}$$

Our simulation result gave the front to back ratio = 5.09764

$$\begin{aligned} \text{So front to back ratio in dbi} &= 10\log (5.09764) \\ &= 7.0736 \text{ dbi} \end{aligned}$$

The decay factor is zero because of our assumption of lossless structure and perfect conduction.

6.5 Construction of the Designed Antenna

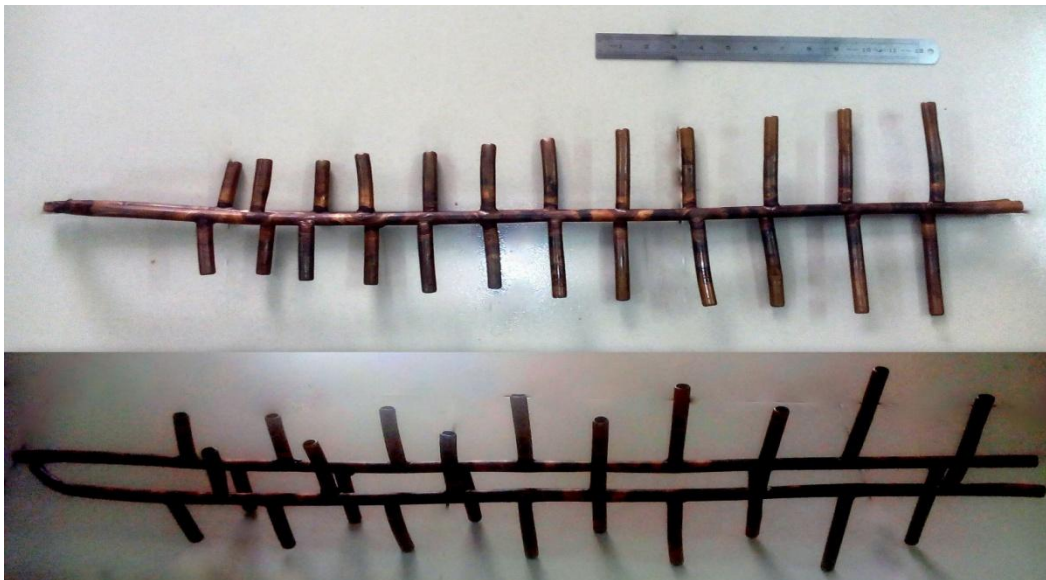


Figure 6.5: Physical structure of the designed LPDA

In figure 6.5 our constructed antenna is shown. The antenna was built using copper material. Each element of the antenna was joined together by gas welding.

CHAPTER 7

CONCLUSION AND FUTURE WORKS

7.1 Conclusion

Initially the concept of Frequency-Independent Antennas is studied. The concept of Log-Periodic Dipole Array antenna has been studied and we have seen that for wideband application log periodic antennas are used. The principle of log periodic dipole antennas (LPDA) requires all the dimensions of the array elements to be scaled in a log periodic manner, to achieve a corresponding scaling in frequencies.

Based on given specifications and for assumed values of Scale Factor (τ) and spacing factor (σ) Log Periodic Dipole Array antenna has been designed.

In this thesis a log-periodic dipole antenna covering a frequency range of 1.35 GHz- 2.69 GHz with required high gain is designed and then simulated by HFSS simulator. In the HFSS, the antenna was drawn using the calculated parameters. The modal solution data report and far field report was observed after the simulation.

Our main goal was to improve the performance of the existing antenna and theoretically we have achieved our aim by designing a high gain (~9 dBi) log periodic dipole antenna (LPDA).

We have also constructed our designed antenna using copper material because of its high conductivity.

7.2 Future Works

Our designed antenna was constructed using copper material. But due to time limitation we couldn't take the field test. So the field performance is still uncertain. In the future this constructed antenna can be tested to compare between the simulated result and field result.

A receiving antenna should be constructed or ensuring optimum transmitting and receiving operation.

In the future, the designed concept can easily be scaled for application with different bandwidth and/or directivity requirements by adjusting angle α and by adding more elements which will also improve the VSWR.

In our simulated result there are some unwanted frequencies which are not in our frequency range. Proper filter can be used to remove these unwanted frequencies.

BIBLIOGRAPHY

- [1]. http://en.wikipedia.org/wiki/Log-periodic_antenna.
- [2]. J. D. Kraus, "Antennas since Hertz and Marconi," *IEEE Trans. Antennas Propagat.*, Vol. AP-33, No. 2, pp. 131–137, February 1985.
- [3]. J. C. Maxwell, *A Treatise on Electricity and Magnetism*, Oxford University Press, London, UK, 1873, 1904.
- [4]. S. Silver (Ed.), *Microwave Antenna Theory and Design*, MIT Radiation Lab. Series, Vol. 12, McGraw-Hill, New York, 1949.
- [5]. *IEEE Transactions on Antennas and Propagation*, Vols. AP-17, No. 3, May 1969; Vol. AP-22, No. 1, January 1974; and Vol. AP-31, No. 6, Part II, November 1983.
- [6]. Constantine A. Balanis , "Antenna Theory", Wiley, third edition,42-43, 2005.
- [7]. Special issue, *IEEE Trans. Antennas Propagat.*, Vol. 34, No. 3, Mar. 1986.
- [8]. Constantine A. Balanis , "Antenna Theory", Wiley, third edition,70-71, 2005.
- [9]. Constantine A. Balanis , "Antenna Theory", Wiley, third edition,94-95, 2005.
- [10]. Kraus, J. D., *Antennas*, 703-710, 2nd Ed., McGraw-Hill, New York, 1988.
- [11]. Mayes, P. E., "Frequency-independent antennas and broadband derivatives thereof," *Proc. IEEE*, Vol. 80, 103-112, Jan. 1992.
- [12]. K. M. Keen, "A planar log-periodic antenna," *IEEE Trans. Antennas Propagation*, vol. AP-22, pp. 489-490, May 1974.
- [13]. R. Carrel, "The design of log-periodic dipole antennas," *IRE Int. Con. Rec.*, 1961, vol. 9, p p. 61-75.
- [14]. R. Carrel, "The design of log-periodic dipole antennas," in *IRE International Convention Record*, 1961, pp. 128.
- [15]. H.-T. Hsu, J. Rautio, and S.-W. Chang, "Novel planar wideband omni directional quasi log-periodic antenna," in *Microwave Conference Proceedings, 2005. APMC 2005. Asia-Pacific Conference Proceedings, 2005*, p. 400.
- [16]. M. N. A Karim, M. K. Abd Rahim, H. A. Majid, O. B. Ayop, M. Abu, and F. Zubir, "Log periodic fractal Koch antenna for UHF band applications," *Progress In Electromagnetics Research*, vol. 100, pp. 201-218, 2010.

- [17]. http://en.wikipedia.org/wiki/Log-periodic_antenna.
- [18]. Q. Abbasi, A. Abbosh, D. Abbott, and W. Abdel- Wahab, "2011 Index IEEE Antennas and Wireless Propagation Letters Vol. 10," IEEE ANTENNAS AND WIRELESS PROPAGATION LETTERS, vol. 10, p. 1615, 2011.
- [19]. R. Carrel, "The design of log-periodic dipole antennas," in IRE International Convention Record, 1961, pp. 61-75.
- [20]. W. L. Stutzman and W. A. Davis, Antenna theory: Wiley Online Library, 1998.
- [21]. http://www.radioelectronics.com/info/antennas/log_p/log_periodic.php.
- [22]. Yi Huang, Kevin Boyle, "Antennas from Theory to Practice", Wiley, 158-159, 2008.
- [23]. P. C. Butson and G. T. Thompson, "A Note on the Calculation of the Gain of Log-Periodic Dipole Antennas," *IEEE Trans. Antennas Propagat.*, AP-24, pp. 105–106, January 1976.